Fresh biochar application provokes a reduction of nitrate which is unexplained by conventional mechanisms

Fresh biochar application provokes a reduction of nitrate which is unexplained by conventional mechanisms

Alba Llovet[1,2], Stefania Mattana[1,10], Juan Chin-Pampillo[1,2,3], Neus Otero[4,5,6], Raúl Carrey[4,5], Claudio Mondini[7], Gabriel Gascó[8], Esther Martí[9], Rosanna Margalef[4,5], Josep Maria Alcañiz[1,2], Xavier Domene[1,2,6], Angela Ribas[1,2]

[1] CREAF, Cerdanyola del Vallès 08193, Spain

[2] Universitat Autònoma de Barcelona, Cerdanyola del Vallès 08193, Spain

[3] Centro de Investigación en Contaminación Ambiental (CICA), Universidad de Costa Rica (UCR), San José, Costa Rica

[4] Grup de Mineralogia Aplicada, Geoquímica i Geomicrobiologia, Departament de Mineralogia, Petrologia i Geologia Aplicada, Facultat de Ciències de la Terra, Universitat de Barcelona (UB), Martí i Franquès s/n, 08020, Barcelona, Spain

[5] Institut de Recerca de l'Aigua (IdRA) de la Universitat de Barcelona (UB), Spain

[6] Serra Húnter Fellowship, Generalitat de Catalunya, Spain

[7] CREA Research Centre for Viticulture and Enology, Via Trieste 23, 34170 Gorizia, Italy

[8] Departamento de Producción Agraria, ETSI Agronómica, Alimentaria y de Biosistemas, Universidad Politécnica de Madrid, Avda. Puerta de Hierro 2, 28040 Madrid, Spain

[9] Laboratori d'Edafologia, Facultat de Farmàcia, Universitat de Barcelona, Av. Joan XXIII s/n, 08028 Barcelona, Catalonia, Spain

[10] Research Group Plants and Ecosystems (PLECO), Department of Biology, University of Antwerp, Wilrijk, B-2610, Belgium

Abstract

Soil-applied biochar has been reported to possess the potential to mitigate nitrate leaching and thus, exert beneficial effects beyond carbon sequestration. The main objective of the present study is to confirm if a pine gasification biochar that has proven able to decrease soil-soluble nitrate in previous research can indeed exert such an effect and to determine by which mechanism. For this purpose, lysimeters containing soil-biochar

mixtures at 0, 12 and 50 t biochar ha^{-1} were investigated in two different scenarios: a fresh biochar scenario consisting of fresh biochar and a fallow-managed soil, and an aged biochar scenario with a 6-yr naturally aged biochar in a crop-managed soil. Soil columns were assessed under a mimicked Mediterranean ambient within a greenhouse setting during an 8-mo period which included a barley crop cycle. A set of parameters related to nitrogen cycling, and particularly to mechanisms that could directly or indirectly explain nitrate content reduction (i.e., sorption, leaching, microbially-mediated processes, volatilisation, plant uptake, and ecotoxicological effects), were assessed. Specific measurements included soil solution and leachate ionic composition, microbial biomass and activity, greenhouse gas (GHG) emissions, N and O isotopic composition of nitrate, crop yield and quality, and ecotoxicological endpoints, among others. Nitrate content reduction in soil solution was verified for the fresh biochar scenario in both 12 and 50 t ha^{-1} treatments and was coupled to a significant reduction of chloride, sodium, calcium and magnesium. This effect was noticed only after eight months of biochar application thus suggesting a time-dependent process. All other mechanisms tested being discarded, the formation of an organo-mineral coating emerges as a plausible explanation for the ionic content decrease.

Keywords: gasification biochar; nitrate mitigation; aging; lysimeters

1. Introduction

Anthropic activity has doubled the pool of reactive nitrogen (N) since pre-industrial times (Vitousek et al., 1997). Intensification of agriculture, and specifically the Haber-Bosch process (synthetic N fixation), and legume cultivation (biological N fixation) greatly contributed to enhanced N fluxes (Galloway et al., 2003). Although N is the main limiting nutrient in non-legume crops, it is estimated that approximately half of all nitrogen applied to boost agricultural production is not taken up by plants but lost to other environmental compartments (Davidson et al., 2011). The main N loss pathways from agroecosystems are: i) nitrate (NO_3^-) leaching, given that NO_3^- is highly soluble in water and thus susceptible to leakage; ii) denitrification, mostly occurring under anaerobic conditions, where NO_3^- is transitorily reduced to nitrite (NO_2^-), then to nitric oxide (NO) and finally to nitrous oxide (N_2O) or dinitrogen (N_2); and iii) ammonia (NH_3) volatilisation, mainly in alkaline soils after organic or NH_4^+-containing fertiliser application. These N losses might not only imply reduced yields but also pose a threat to environmental and human health e.g., high levels of NO_3^- in water

resources have been linked to sanitary problems such as cancer and methemoglobinemia (Powlson et al., 2008; Ward et al., 2018) and environmental adverse effects as eutrophication; N_2O is a potent greenhouse gas (GHG) with 265 times the warming potential of carbon dioxide (IPCC, 2014); and NH_3 volatilisation can cause damage to sensitive crops (Pearson & Stewart, 1993), led to acidification (Cameron et al., 2013), and act as a secondary source of nitric and nitrous oxides (Bowman, 1990).

Therefore, there is an urge to develop mitigation strategies to cope with elevated N fluxes, and biochar amendment to soil has arisen as a valuable option. Biochar is the solid by-product of biomass pyrolysis or gasification i.e., thermal decomposition in zero or very low oxygen conditions (Sohi et al., 2010). Biochar is characterised by its polycondensed aromatic carbon backbone, a high surface area provided by its porous structure, and the abundance of reactive functional groups on its surface. Those properties have been reported to translate into a high C stability (and therefore C sequestration potential), and an increased nutrient and water retention capacity (Glaser et al., 2016). Physicochemical properties of biochar are highly dependent on the biomass feedstock and the pyrolysis procedure used (especially temperature), and its practical effects in the field can further vary as a result of application rates, climate conditions, soil properties, crop type, and residence time in soil (Joseph et al., 2010; Nguyen et al., 2017). Furthermore, the inner complexity of the soil nitrogen cycle leads to a variety of mechanisms in which biochar addition can alter N transformations. This is why many inconsistencies on the biochar effect on N fluxes are found in the literature, either increasing or diminishing them, as well as having no effects at all (Clough et al., 2013). Despite the aforementioned disparity, numerous studies have pointed out biochar's ability to reduce NO_3^- leaching (Dempster et al., 2012; Kammann et al., 2015; Ventura et al., 2013; Yao et al., 2012). The principal suggested mechanisms comprehend sorption, microbial N-cycling shifts (including immobilisation, mineralisation, nitrification and denitrification), and NH_3 volatilisation among others, described hereafter.

Sorption of NH_4^+ through biochar's cation exchange capacity (CEC) is a classic proposed mechanism to explain nitrogen retention (Lehmann et al., 2003; Liang et al., 2006; Nelissen et al., 2012), which is expected to intensify over time leading to a larger nutrient retention in aged as opposed to fresh biochar (Kookana et al., 2011). Conversely, NO_3^- sorption by anion exchange capacity (AEC) is restricted to few examples (Lawrinenko & Laird, 2015), but other mechanisms such as bridge bonding (Mukherjee et al., 2011), non-conventional ion-water bonding and non-conventional hydrogen bonding (Conte et al., 2014; Kammann et al., 2015) have been suggested to explain direct NO_3^- retention.

88 Regarding microbial N-cycling, biochar could alter it in multifarious pathways. It has been reported that the
89 labile C pool present in fresh biochars can cause a transitory increase in soil microbial biomass shortly after
90 being applied, leading to a simultaneous C and N retention in microbial biomass (Ippolito et al., 2012). N
91 mineralisation and nitrification can decrease with biochar addition as a result of toxic effects (Clough et al.,
92 2010), or as inorganic N is retained and excluded from metabolic routes (Pal, 2016). Biochar can also affect
93 whether denitrification is favoured, as this process is stimulated in anaerobic conditions, and biochar can
94 influence water-filled pore space, and, in turn, oxygen supply (Hagemann et al., 2016).
95 Finally, NH_3 volatilisation, associated to the liming effect of some biochars, is a proposed N loss path
96 (Schomberg et al., 2012) whereas NH_3 adsorption onto biochar is also possible (Asada et al., 2006; Doydora
97 et al., 2011), which can indeed lead to enhanced plant N uptake (Mandal et al., 2016; Taghizadeh-Toosi et al.,
98 2012).
99 Previous studies of our research group have pointed out a reduction of the soluble NO_3^- topsoil content in
100 outdoor biochar-amended mesocosms under Mediterranean conditions fifteen months following the
101 application (Marks et al., 2016) but the mechanism responsible for that reduction was not ascertained.
102 Therefore, the aims of this study were to: i) prove that biochar is effective in reducing nitrate concentrations
103 at short- and long-term, and ii) determine which one of the above explained mechanisms is mainly operating.
104 For this purpose, N-pools were monitored for 8 months in greenhouse lysimeters mimicking a plant-soil system
105 using two biochar supplementation scenarios (freshly added biochar and biochar naturally aged in soil for 6
106 years), applied at three addition rates (0, 12 and 50 t ha^{-1}).
107

108 **2. Materials and methods**

109 **2.1. Lysimeter setup**

110 A lysimeter system was set up in a greenhouse setting at the IRTA Torre Marimón experimental station (Caldes
111 de Montbui, NE Spain) to simulate the effects of biochar agricultural amendment at increasing application
112 rates (0, 12 and 50 t ha^{-1}, which corresponded to 0, 37.7, and 157.1 g of biochar per lysimeter), and at two
113 contrasted ageing scenarios: just after the biochar application (fresh), and 6 years after natural ageing of biochar
114 in outdoor soil mesocosms (aged). The biochar used in this experiment was produced from *Pinus pinaster* and

115 *P. radiata* wood chips within a gasification reactor (600-900ºC) with a residence time of 10 s (see biochar
116 physicochemical characterisation summarised in **Table 1**). For a more detailed description on the biochar
117 preparation refer to Marks et al. (2014a).

118 Each lysimeter consisted of a polyvinyl chloride (PVC) tube (48 cm height x 20 cm diameter) with a perforated
119 lid in the bottom, which was covered with a 2mm-mesh gauze and a 2 cm quartz sand layer to ensure proper
120 drainage without substantial soil loss. Then, two 20 cm layers of soil (6.7 kg each) were added to mimic B and
121 Ap horizons, the former consisting of only soil, and the latter of soil-biochar mixtures. The soil used for the
122 lysimeters construction corresponded to a *Fluventic Haploxerept* (Soil Survey Staff, 2010) described in detail
123 in Marks et al. (2016), but two differentially managed soils within the same field were used according to the
124 different biochar ageing scenarios. A soil portion that has been under fallow since 2011 was either used as B-
125 horizon for all the lysimeters and also to prepare soil-biochar mixtures used as Ap-horizon in the lysimeters of
126 the fresh biochar scenario. Instead, for the aged biochar scenario, the Ap horizon corresponded to the topsoil
127 (20 cm) of outdoor mesocosms of the experiment described in Marks et al. (2016). The mesocosms were set
128 up in March 2011 and therefore contained biochar aged for six years. Also, the mesocosms had been fertilised
129 with pig slurry at a 50 kg N ha^{-1} $year^{-1}$ rate and cropped to barley all over this period. In summary, two different
130 biochar scenarios, fresh (F) and aged (A), and three addition rates (0, 12 and 50 t ha^{-1}) were tested, yielding a
131 total of six treatments hereafter designated as A_0, A_{12}, A_{50}, F_0, F_{12}, and F_{50}, assigned in a fully replicated (n =
132 5) randomised design.

133 The lysimeters were set up on 23rd March 2017 and left to stabilise for 11 days after an initial watering. On 3rd
134 April fifteen barley seeds (*Hordeum vulgare*) were sown (later thinned to only 1 plant per lysimeter), and each
135 lysimeter was fertilised with 7.3 g of a thermally dried pig slurry which corresponded to a 100 kg N ha^{-1}
136 addition rate based on the available N (see pig slurry characterisation in **Supplementary Table S1**). A drip
137 irrigation system was installed on each lysimeter to keep moisture around 50% of the maximum water holding
138 capacity (i.e., 16.5% moisture w/w) during barley growth. After harvest (on 3rd July) a drought period was
139 simulated in order to mimic the Mediterranean climate. Only three spaced irrigation events were performed
140 during summer and early fall, which coupled to the high temperatures in the greenhouse, led to dry soil
141 conditions during most of the period. Drought conditions were suppressed to some extent shortly before the

final sampling, with a fourth irrigation event coupled to lower temperatures (records of greenhouse temperature and lysimeters moisture are shown in the **Supplementary Figure S1**).

Soil physicochemical, microbial, and isotopic parameters were assessed at five samplings along 2017, each corresponding to relevant stages in terms of fertilisation and plant development: pre-fertilisation (3rd April); post-fertilisation (5th April); developed plant (7th June); harvest (5th July) and bare soil (4th December) (**Supplementary Figure S1**). GHG soil emissions were assessed at the same dates except for the pre-fertilisation sampling, carried out at 30th March instead of 3rd April, and that of the developed plant stage, which was substituted by an earlier one (12th April) taken as additional post-fertilisation sampling in order to cover the possible gas emission peaks after fertilisation.

2.2. Soil physicochemical analyses

2.2.1. Soil extract analyses: water-soluble and exchangeable ions, pH, moisture and electrical conductivity

A 5.5x7 cm core was used to collect soil samples in each lysimeter, then soil was manually homogenised in a plastic bag. KCl extracts were immediately prepared in the greenhouse on a 1:5 w/v ratio by mixing 20 g of fresh soil with 100 ml of 2 M KCl. Once in the laboratory, 1:5 ratio (w/v) water extracts were prepared by mixing 40 g of soil with 200 ml of distilled water and by shaking for 1 h in a vertical agitator (120 rpm) whereas KCl extracts were shaken for 30 min (ISO/TS 14256-1: 2003). In parallel, 10 g of soil were used for moisture determination. Both KCl and water extracts were centrifuged for 5 min at 8000 rpm, filtered in Whatman #42 filter paper, and frozen at -20 °C for later determination of ion content. Before freezing, a portion of the water extracts was used for pH and electrical conductivity (EC) measurement. Water-soluble ionic concentrations were determined by liquid chromatography on a Dionex ICS-1100 ion chromatograph (Dionex, Sunnyvale, USA) using a AS4A-SC Dionex anion column for Cl^-, NO_2^-, NO_3^-, HPO_4^{2-} and SO_4^{2-} determination and a CS12A Dionex cation column for Na^+, K^+, Mg^{2+}, and Ca^{2+} determination. All the ion concentrations were estimated using linear calibration except for SO_4^{2-}, Mg^{2+}, and Ca^{2+} in which quadratic regression substantially increased fitting (R^2). Detection limit (LOD) estimation was stipulated as three times the standard deviation of five blank values. Exchangeable $N\text{-}NH_4^+$ was assessed by subtracting water extractable concentrations to KCl extractable concentrations. For comparability purposes, both KCl and water extractable $N\text{-}NH_4^+$ were

measured using the salicylate method (Willis et al., 1996), in a Spectronic 20 Genesys 4001/4 spectrophotometer. To validate the possibility of nitrate bridge bonding mechanisms later discussed, KCl-extractable NO_3^- was determined following Matsumura et al. (1999), but only for the bare soil sampling. It was found that increasing the volume sample up to 1 ml (instead of the recommended 0.1 ml in Willis et al. (1996)) for N-NH_4^+ determination in KCl and water extracts increased sensitivity without interferences, and for N-NH_4^+ determination after Kjeldahl digestions of soil and K_2SO_4 extracts (see below) sample volumes were set at 0.3 and 0.5 ml, respectively.

2.2.2. Soil total Kjeldahl nitrogen and organic carbon

A portion of the collected soil was air-dried and finely grounded (ø < 0.2 mm) in order to assess Kjeldahl nitrogen and organic carbon. Total Kjeldahl nitrogen (TKN) was assessed using the micro-Kjeldahl method by Bremner (1965) with the following modifications: after digestion was finished, digestates were diluted with distilled water to make up a volume of 100 ml and N-NH_4^+ was measured by the salicylate method. Organic carbon was determined by the Walkley–Black $K_2Cr_2O_7$-H_2SO_4 oxidation method (Nelson & Sommers, 1983).

2.2.3. Leachates

After soil sampling, an irrigation-induced leaching was carried out by placing each lysimeter on a glass tray but suspended 1.3 cm above its surface to allow drainage. The water addition needed to produce a leachate volume of c.a. 200 ml was estimated by measuring lysimeters water content gravimetrically, and taking into account trials before the lysimeters setup that enabled us to estimate the water holding capacity around 24%. This procedure allowed the calculation of the total volume of water in the system (soil water content + water added to provoke leaching) required to express leachate analysis on a dry basis. In the laboratory, the obtained leachates were filtered and analysed by liquid chromatography as described for water extracts (except for ammonium measurement, which was also undergone by chromatography instead of the salicylate method).

2.3. Soil microbial analyses

A subsample of the fresh soil batch previously described was used to determine microbiological endpoints. Soil basal respiration (BAS) was assessed with CO_2 traps according to Pell et al. (2006). Microbial biomass-

carbon (C_{mic}) and nitrogen (N_{mic}) were obtained using the chloroform fumigation-extraction method (Vance et al., 1987). In detail, 10 g of soil fresh weight (FW) corresponding to the fumigated samples were exposed to a chloroform-saturated atmosphere (fumigated) by placing the samples in a hermetically closed desiccator and by boiling 50 ml of chloroform placed in a 100 ml beaker under vacuum for 2 minutes and then closing the desiccator seal for 24 h. Both the unfumigated and fumigated samples were then mixed with 0.5 M K_2SO_4 at a 1:4 soil:solution ratio, vertically shaken for 120 minutes, and the extracts filtered through Whatman #42 filter paper. C_{mic} was determined by wet oxidation of an extract aliquot with potassium dichromate followed by titration with Mohr's salt, and estimated as the difference in C concentration between fumigated and non-fumigated soil divided by K_{EC} = 0.38 (Vance et al., 1987). N_{mic} was assessed by a Kjeldahl digestion of an extract aliquot coupled to salicylate N-NH_4^+ determination explained in Cabrera and Beare (1993). The difference in the Kjeldhal N concentration in between fumigated and non-fumigated soil, divided by K_{EN} = 0.5 (Voroney et al., 2008), was used to calculate N_{mic}. Although N_{mic} is generally estimated using the total nitrogen in K_2SO_4 extracts (therefore including N-NH_4^+ but also N-NO_2^- and N-NO_3^- concentration), we used Kjeldahl nitrogen instead (organic nitrogen plus inorganic N-NH_4^+) since nearly all the nitrogen in microorganisms is organic. N_{mic} of the post-fertilisation sampling was not considered due to the negative values found in many lysimeters which are plausibly an artefact related to the elevated and heterogeneous concentrations of inorganic NH_4^+ in both fumigated and unfumigated samples, sampled two days after the pig slurry application. The calculation of N_{mic} for the F_0 treatment at the bare soil sampling was also elusive as the high nitrate levels in the F_0 treatment interfered with Kjeldahl measurement, since NO_3^- can undergo reaction with NH_4^+ to form N_2O during digestion. Even when assessed with the pre-treatment proposed by Wyland et al. (1994) such interference persisted, as shown by values below the analytical blanks. For this reason, N_{mic} of the mentioned treatment was also measured with the ninhydrin method (Brookes & Joergensen, 2006).

The organic carbon and Kjeldahl nitrogen in K_2SO_4 extracts of the unfumigated samples were taken as dissolved organic C and N (DOC and DON).

2.4. Gas sampling: N_2O, CO_2, NH_3

Trace gas emissions of N_2O and CO_2 were evaluated employing non-flow-through, non-steady-state chambers. The gases were collected according to the methodology of Collier et al. (2014) and using static chambers (21.5

cm high, 21 cm diameter) with a vent to prevent pressure gradients influencing gas exchange. For emission rates estimation, gases were accumulated in the chamber and air samples were collected at three time points: one taken immediately after chamber closure (t= 0), and after 10 and 20 min or after 15 and 30 min, as chamber deployment duration was prolonged in samplings when air temperature was cooler. It is recommended (De Klein and Harvey, 2015) that chamber height (cm) to deployment time (h) ratio should be ≥40 cm h^{-1}, in our case it was 64.5 cm h^{-1} for 20 min deployment duration and 43 cm h^{-1} for 30 min deployment duration. Gas samples were extracted from the static chambers using a plastic syringe (20 ml) and injected into a 12 ml vial (Exetainers®, Labco Ltd., Ceredigion, UK), and then analysed by gas chromatography (Agilent 7890A) coupled to ECD and TCD. The detection limits of the GC are 10 ppmV and 20 ppbV for CO_2 and N_2O, respectively. Quality of analysis was checked using standards of known gas concentrations (250 and 1003 ppmV for CO_2 and 175 and 600 ppbV for N_2O). Fluxes were calculated from the slope of the linear regression between the concentration of each GHG and the accumulation time inside the chamber, subsequently corrected by the air temperature, the atmospheric pressure, and the surface-volume ratio of the chamber, as described in detail by Barton et al. (2008). The Pearson R^2 coefficient corresponding to the concentration of CO_2 accumulated in a linear and increasing manner was used as an indicator that the system was functioning properly. This is why the N_2O fluxes were only considered when the CO_2 fluxes had an $R^2 \geq 0.80$.

NH_3 emissions were measured by chemical traps, which consisted of 10 ml of a 0.5% (w / v) boric acid solution, placed in 50 ml plastic cups, containing 3 drops of indicator (0.099 g of bromocresol green and 0.066 g of methyl red dissolved in 100 ml of 96% ethanol). A trap was placed at each lysimeter soil surface and then the lysimeter sealed with a polyethylene sheet to allow NH_3 accumulation and its capture in the traps. Cups were only collected when the indicator colour changed from pink to green and the time registered. At collection, each trap was closed with a lid and transported to the lab for its titration with 1 mM HCl for the NH_4^+ concentration estimation. These measurements were only carried out around the fertilisation event, with non-detectable NH_3 concentrations in a pre-fertilisation accumulation period of 91 h, and detectable levels only in the 9 days following fertilisation as represented by four samplings with accumulation times ranging between 19 and 46 h.

2.5. Isotopic composition analyses

Isotopic composition analyses were performed in lysimeters' soil KCl extracts (for treatments A_0, A_{50}, F_0, and F_{50}) and leachates (for treatments F_0 and F_{50}). Ancillary measurements included the determination of the $\delta^{15}N$ and $\delta^{18}O$ of dissolved NO_3^- from irrigation water at two different dates (3rd April 2017 and 4th December 2017), and of the bulk $\delta^{15}N$ of soil (F_0, F_{50}, and A_{50}), harvested barley stem and leaves (F_0, F_{50}), biochar, and pig slurry. The $\delta^{15}N$ and $\delta^{18}O$ of dissolved NO_3^- were determined using a modified cadmium and azide reduction method (McIlvin and Altabet, 2005; Ryabenko et al., 2009) followed by a simultaneous $\delta^{15}N$ and $\delta^{18}O$ analysis of resultant N_2O using a Pre-Con (Thermo Scientific) coupled to a Finnigan MAT-253 Isotope Ratio Mass Spectrometer (Thermo Scientific). The bulk $\delta^{15}N$ of soil, plant, biochar, and pig slurry samples was determined in a Carbo Erba EA-Finnigan Delta C IRMS. Following Coplen (2011), several international and laboratory (UB) standards were interspersed among samples for the normalisation of the isotope results i.e., USGS-32, USGS-34, USGS-35, UB-IWS_{NO3} ($\delta^{15}N$ = +16.9 ‰, $\delta^{18}O$ = +28.5 ‰) for the $\delta^{15}N$ and $\delta^{18}O$ of dissolved NO_3^-; and USGS-40, IAEA-N1, IAEA-N2 and UCGEMA-P, for the $\delta^{15}N_{bulk}$ of solid materials. The standard deviation reproducibility of the samples was ±1.0 ‰ for $\delta^{15}N$ of dissolved NO_3^-; ±1.5 ‰ for $\delta^{18}O$ of dissolved NO_3^-; and ±0.2 ‰ for $\delta^{15}N_{bulk}$ of solid materials. Values of $\delta^{15}N$ are reported relative to Atmospheric (AIR), and $\delta^{18}O$ values are reported relative to Vienna Standard Mean Ocean Water (V-SMOW) in per mill (‰) as defined by equations a and b:

$$\delta^{15}N_{NO_3} = \left[\frac{\left(\frac{^{15}N}{^{14}N}\right)_{sample} - \left(\frac{^{15}N}{^{14}N}\right)_{AIR}}{\left(\frac{^{15}N}{^{14}N}\right)_{AIR}}\right] \quad (a)$$

$$\delta^{18}O_{NO_3} = \left[\frac{\left(\frac{^{18}O}{^{16}O}\right)_{sample} - \left(\frac{^{18}O}{^{16}O}\right)_{VSMOW}}{\left(\frac{^{18}O}{^{16}O}\right)_{VSMOW}}\right] \quad (b)$$

2.6. Plant yield and nutrient uptake

Above-ground barley biomass was harvested at the end of its life cycle in early summer (3rd July, 2017) and dried at 60ºC for 48 h. Growth parameters assessed were straw and grain weight, ear count, and mean number of grains per ear. After straw and grain grinding in a ball-mill, nutrient content (N, P, K, Ca, Mg, S, Mn, and Zn) was obtained by near infrared spectrometry (NIRS) by scanning the grounded samples in duplicate from 1100 to 2500 nm using a NIRSystems 5000 scanning monochromator (FOSS, Hilleröd, Denmark) employing the calibrations developed in a previous study (Martos et al., 2020).

2.7. Ecotoxicological characterisation

Subsamples from each soil and soil-biochar mixtures were taken before lysimeters setup to be used for the ecotoxicity assessment. On the one hand, the collembolan *Folsomia candida* was used as a proxy of toxicity to soil organisms using the survival and reproduction test of the ISO Guideline 11267 (ISO 1999).

On the other hand, elutriates from the soil and soil-biochar mixtures were prepared to assess aquatic toxicity, mimicking the potential exposure of aquatic organisms to runoff. For this purpose, growth inhibition of the algae *Raphidocelis subcapitata* (SAG 61.81, Inst. Plant Physiology U. Göttingen) was tested following OECD 201 (2011). Specifically, yield inhibition rate (72 h) was assessed at four elutriate dilutions (81.6, 51, 30.6, and 10.2 % v/v) of an initial elutriate prepared as follows: a 1:10 (w/v) soil-water mixture suspension (25 g of air-dried soil: 250 ml of water) was prepared, stirred for 12 h in a vertical agitator (120 rpm), and centrifuged 20 minutes at 10000 rpm. Then, centrifuge tubes were decanted to collect the supernatants, kept refrigerated until testing before 24 h. The used method is a modification of the DIN 38414_S4 (1984), since a higher centrifugation speed was used to reduce the turbidity caused by biochar particles in the suspension (from 4500 to 10000 rpm).

Finally, potential impacts on nitrogen-related microbial functional groups were assessed at the 12th April 2017 sampling (9 days after fertilisation), when a microbial activity peak was expected, so as to detect any ecotoxicological effects. The target functional genes assessed were: amoA for the ammonia-oxidizing bacteria (AOB) and archaea (AOA); nxrB for the beta subunit of nitrite oxidase of Nitrobacter sp.; nirK and nirS for NO_2^- reducers to gaseous nitric oxide carrying a nitrite reductase enzyme; nosZ for denitrifiers carrying the nitrous oxide reductase enzyme; and nifH for N_2-fixing microbes to reduce it to NH_4^+. Fresh soil samples stored at -80 °C were used for simultaneous extraction of DNA and RNA following the protocol described in

Griffiths et al. (2000) with the modifications provided by Töwe et al. (2011). Nucleic acids were quantified with the Qubit 3.0 Fluorimeter (Life Technologies) as instructed by manufacturer. Retro RNA transcription was performed using All-in-One cDNA Synthesis SuperMix (Bimake) following the manufacturer's protocol. The real-time PCR (quantitative PCR indicated as qPCR) was carried out in the UAB Campus Agrogenomic Service, with a LightCycler® 480 System (Roche). **Supplementary Table S2** shows more details of the qPCRs of the quantified functional genes. All the samples and standards were analysed in duplicate and each plate contained 6 negative control replicates. The amplification efficiency was calculated as: E = [10 (-1 / slope) -1] * 100, was and the results were: nifH: 87-93%; bacterial amoA: 88-93%; archaeal amoA: 87-93%; nxrB: 97-99%; nirK: 97-99%; nosZ: 86-90% and nirS: 82-84%. These efficiency values are consistent with those reported in the literature by similar studies (Töwe et al., 2010; Harter et al., 2014).

2.8. Statistical tests

The statistical treatment of the experimental data was carried out using R software v. 3.6.1 (R Core Team, 2019), and its visualisation using the packages *ggplot2* (Wickham, 2016) and *ggpubr* v 0.2.3 (Kassambara, 2019a). Fresh and aged-biochar treatments were always tested separately since their corresponding controls were found to differ significantly in key properties such as organic carbon and Kjeldahl nitrogen as expected by the different starting points of each scenario (six years of fallow in the fresh biochar scenario and continuous cropping in the aged biochar scenario).

Longitudinal data (i.e., variables for which exist a between-subjects factor = biochar addition rate, and a within-subjects factor = different sampling dates) were analysed using two-way mixed ANOVAs, which were computed with the *rstatix* package v0.2.0 (Kassambara, 2019b). Shapiro-Wilk and Levene tests were used to ensure normal distribution and homogeneous variances, respectively. When these assumptions were not met, the test was run on the $\log_{10}$-transformed variable. The assumption of sphericity was checked using the Mauchly's test and when violated the Greenhouse-Geisser correction was applied. Finally, homogeneity of covariances was tested by Box's M. Statistical results of the mixed ANOVA are shown in **Supplementary Table S3 (S3.1.-S3.36.)**. Pairwise comparisons were tested with t test with Bonferroni adjustment, and the significance level was set at $p < 0.05$.

By contrast, parameters analysed at a single sampling date were assessed by means of the Kruskal–Wallis test followed by pairwise comparisons with the Wilcoxon's test with Bonferroni adjustment (*rstatix* package v 0.2.0 (Kassambara, 2019b)) since the low n values resulted insufficient to ensure that requirements for parametric tests were being met. For tests that only involved two independent groups, the Mann-Whitney-Wilcoxon test with Bonferroni adjustment was used. In the provided graphs, significant differences between biochar-amended and control lysimeters are indicated by lower case letters. Hereafter within the text, all values are reported as mean ± standard error (SE).

3. Results

3.1. Soil physicochemical parameters

Results for moisture, EC, pH, Total Kjeldahl Nitrogen (TKN), and C_{org} are presented in **Figure 1**. Biochar application significantly increased C_{org} in both fresh and aged biochar scenarios throughout the entire experiment. While in the fresh biochar scenario the increase of C_{org} was proportional to biochar application rate, in the aged biochar scenario the difference between 12 and 50 t ha^{-1} was less marked. Regarding the remainder parameters, significant biochar effects were only found in the fresh biochar scenario: i) moisture levels were significantly enhanced at two sampling dates (5th April and 5th July), with a non-significant increase at 4th December, the effect being more pronounced in the F_{50} treatment than in F_{12}; ii) EC was higher in the F_{50} treatment compared to F_0 at the pre-fertilisation sampling (3rd April), whereas this trend reverted at the bare soil sampling (4th December), being F_0 the treatment with highest values; iii) F_{50} treatment lead to significant higher TKN at one sampling date (7th June) with respect to control. It has to be pointed out that TKN measured at 4th December (a date with high levels of N-NO_3^-) is misleading since we observed important inconsistencies between total nitrogen (measured by combustion) and the sum of TKN plus (NO_3^- +NO_2^-)-N in F_0 and F_{50} treatments (data not shown). As Bremner & Mulvaney (1983) reported, soils with significant amounts of NO_3^- and NO_2^- present unexpected problematics in total N analysis, since the usually employed Kjeldahl methods do not quantitatively recover N-NO_3^- and N-NO_2^-, but they usually include some of this N. Finally, regarding soil pH, it was unaffected by any of the treatments.

Concerning N species, concentrations of N-NO_2^- and N-NH_4^+ were below detection limits in all the leachates, as also found for N-NO_2^- in all the water extracts except in the post-fertilisation sampling. N-NO_3^- was the

dominant inorganic N form in soil extracts and leachates along the different sampling dates with exception of the post-fertilisation sampling (5th April), where total (soluble + exchangeable) $N\text{-}NH_4^+$ outnumbered $N\text{-}NO_3^-$ in soil extracts (**Supplementary Figure S2**). $N\text{-}NO_3^-$ concentration in soil extracts only differed significantly as affected by biochar addition at the bare soil sampling in fresh biochar treatments. Namely, a significant decrease in $N\text{-}NO_3^-$ content in F_{12} (-69 %) and F_{50} (-64 %) with respect to control was observed (**Figure 2**). In order to confirm this result, a Kruskal-Wallis H test was performed excluding one extreme outlier present in the F_0 treatment. Statistical significance remained ($\chi^2_{(2, N = 14)} = 6.53$, $p = 0.04$), but results of the Bonferroni post hoc test were not sufficient to make statements about pair-wise differences. Since $N\text{-}NO_3^-$ availability reduction still showed an important magnitude effect for both F_{12} and F_{50}, -57 % and -51 % respectively, it was concluded that the effect is consistent. Furthermore, this trend was also shown for another anion (Cl^-), several cations (Ca^{2+}, Mg^{2+}, Na^+), and DOC (**Figure 3**), with significant differences among treatments shown in **Supplementary Figure S3** for ionic species, and in the **Supplementary Figure S4** for DOC. We found that those concentration reductions are more robust in the F_{12} treatment for some ionic species and that the differences in DOC, although following the same tendency, are not significant. Other ions such as K^+, SO_4^{2+}, $N\text{-}NO_2^-$ and $N\text{-}NH_4^+$ didn't show this trend. HPO_4^{2-} is not shown as its signal-to-noise ratio in the chromatogram didn't exceed the set value of 3.

It is also worth noting that although $N\text{-}NO_3^-$ increased its concentration at the bare soil sampling, the proportion of losses as leaching decreased at this sampling, especially for the F_0 treatment. Specifically, $N\text{-}NO_3^-$ leachate content for F_0 treatment represented a 10% of the $N\text{-}NO_3^-$ soil solution content while for F_{12} a 20% and for F_{50} a 25% (**Supplementary Figure S2**). N-forms in leachates did not show significant differences between treatments (**Figure 2**, **Supplementary Figure S3**) although a trend to increased ionic content can be observed for the F_{50} treatment.

In relation to exchangeable N forms, $N\text{-}NH_4^+$ only exhibited an important peak at the post-fertilisation sampling (5th April) (**Supplementary Figure S5**). At this date there were no significant differences due to treatment although an inverse trend was observed between ageing scenarios: while in the fresh biochar scenario biochar treatments surpass control in exchangeable $N\text{-}NH_4^+$ concentrations, the opposite is true in the aged biochar scenario. At the 5th July sampling F_{50} had significantly larger concentrations (2.53 ± 0.31 mg kg^{-1}) than F_{12} (1 ± 0.2 mg kg^{-1}). KCl-extractable $N\text{-}NO_3^-$ didn't significantly exceed water-soluble $N\text{-}NO_3^-$ (**Supplementary Figure S6**) and showed a significant reduction in F_{12} treatment (278 ± 27.6 mg kg^{-1}) and a

non-significant reduction in F_{50} treatment (315 ± 60.5 mg kg^{-1}) compared to F_0 (752 ± 217.4 mg kg^{-1}) after a Kruskal Wallis H test ($\chi^2_{(2, N = 15)} = 7.98$, $p = 0.02$).

Finally, DON (**Supplementary Figure S4**) is not discussed due to the methodological issues previously explained in section 3.2 that hindered its estimation for the F_0 treatment at the bare soil sampling.

3.2. Soil microbial analyses

None of the microbial parameters was significantly affected by any biochar treatment (**Table 2**) with the exception of an increased BAS value in the A_{50} treatment in comparison with A_0 at the harvest sampling date (7th June). Unfortunately, we could not properly measure N_{mic} for F_0 treatment at the bare soil sampling (4th December) by Kjeldahl means due to the methodological issues explained in section 2.3. Although ninhydrin method has been proved useful to determine the presence of N in this treatment, the obtained value (24.1 ± 2.35 mg kg^{-1}) is not shown in the table as this method underestimates N_{mic} compared to Kjeldahl method (Hedqvist & Udén, 2006).

3.3. Gas emission rates: N_2O, NH_3, and CO_2

Gas emission rates results are summarised in **Figure 4**. Regarding the mixed ANOVA results of N-N_2O emissions, there were no significant main effects of treatment although a significant interaction of treatment with time occurred in both fresh and aged biochar scenarios (**Supplementary Table S3.30**). Nevertheless, t-tests between treatments within the different dates were not sufficient to make statements about pair-wise differences. However, some inverse non-significant trends can be observed. Namely, at the 12th April sampling, when emissions peaked, there was a trend to increased emissions for 12 t ha^{-1} and less markedly for 50 t ha^{-1} compared to 0 t ha^{-1} in both fresh and aged biochar scenarios, whereas at 5th April, only 7 days before, the control surpassed biochar treatments in both scenarios.

NH_3 was only detectable during a 9-day period after the fertilisation event. Despite the lack of statistical significance on N-NH_3 emissions between treatments, it can be observed a sustained tendency for higher emissions in F_{12} than F_0 and $F_{50,}$ while in the aged biochar scenario this trend is less marked.

Finally, soil C-CO_2 emissions were significantly reduced by the F_{50} treatment with respect to control at the post-fertilisation 12th April sampling date, while in the previous sampling date (5th April), which is also described as post-fertilisation, F_0 also shows a non-significant trend to highest C-CO_2 emission rates.

3.4. N and O isotopic composition of NO_3^- in KCl extracts and leachates in the fresh biochar scenario

Concerning N and O isotopic composition of NO_3^- in KCl extracts, there was a lack of significant variations due to biochar treatment. Nevertheless, some temporal trends can be observed. In the pre-fertilisation sampling (3rd April), δ^{15}N-NO_3 values of control and biochar lysimeters fell between the observed range of soil N (+5 to +6.8 ‰) (**Figure 5**). After fertilisation (5th April), the value of δ^{15}N-NO_3 slightly decreased. Later, in summer (7th June and 5th July), values of δ^{15}N-NO_3 increased in all treatments, and in the F_0 treatment this was coupled to an increase in δ^{18}O-NO_3 (in the F_{50} treatment, the δ^{18}O-NO_3 also increased on 7th June but not on 5th July). Finally, on 4th December, δ^{15}N-NO_3 values evolved towards to the pre-fertilisation values. **Supplementary Figure S7** shows the isotopic composition of aged KCl extracts, which presented a similar temporal pattern to that of the fresh ones.

Regarding leachates, they presented lower variability in δ^{15}N-NO_3 than KCl extracts but a similar temporal trend. δ^{18}O-NO_3 showed inverse tendencies with respect to KCl extracts between treatments: whereas in KCl extracts the δ^{18}O-NO_3 was lower in the F_0 compared to the F_{50} treatment on 3rd April, 5th April , 7th June and 4th December, for the leachates the opposite is true. There was a remarkable effect of biochar treatment in δ^{18}O-NO_3 of leachates, namely F_0 treatment showed significant higher δ^{18}O-NO_3 values than F_{50} throughout all the sampling dates. Maybe the influence of δ^{18}O-NO_3 of the irrigation water, which was quite high (+6.6 to +7.2 ‰), was higher in F_0, raising its values. Conversely, since F_{50} possessed an enhanced water content, the effect of irrigation water could be diluted.

3.5. Plant nitrogen export and growth parameters

Neither growth parameters nor N plant export showed any significant difference due to biochar treatments. **Table 3** shows these endpoints including three lysimeters that presented underdeveloped plants: two replicates of the A_{50} treatment and one of the A_{12} treatment, although we were unable to identify if this was due to treatment effects or other factors. At the 5th July sampling, those lysimeters showed a three-fold increase in NO_3^- concentrations in water extracts and leachates compared to the ones with well-developed plants, which were attributed to a decreased plant uptake. Since nitrate content differences between underdeveloped and well-developed plants did not represent statistically significant differences, the underdeveloped plant NO_3^- data were not excluded from the soil extracts and leachate analyses. In addition, the uptake of other nutrients besides N was also studied (**Supplementary Table S4**) again without any remarkable biochar effect.

3.6. Ecotoxicological endpoints

435 Regarding the ecotoxicity of soil and soil elutriates of the soil-biochar mixtures collected before lysimeters
436 setup, and despite a slight trend indicating toxicity for F_{50} treatment, no significant effect on adult survival and
437 reproduction were found neither for *Folsomia candida* (**Supplementary Table S5**), nor in the growth
438 inhibition test with *Raphidocelis subcapitata* (**Supplementary Table S6**).

439 Concerning the impacts on microbial functional groups related to N-cycle shortly after fertilisation (12th April),
440 not a single significant difference was obtained, although the number of gene transcripts involved in the
441 nitrification process, i.e., bacterial amoA (AOB), archeal amoA gene (AOA) and nxrB, showed a trend to
442 decrease in F_{12} treatment (**Supplementary Figure S8**).

443

444 **4. Discussion**

445 **4.1. Fresh biochar treatments mitigated nitrate and other ion concentrations at the bare soil sampling**

446 Considering both controls (F_0, A_0) and biochar treatments (F_{12}, F_{50}, A_{12}, A_{50}), two different dynamics in soluble
447 ion concentrations could be distinguished. Namely, K^+, SO_4^{2-}, N-NO_2^- and N-NH_4^+ showed highest
448 concentrations following fertilisation, with N-NO_2^- and N-NH_4^+ having negligible concentrations throughout
449 the rest of the samplings, while N-NO_3^-, Cl^-, Ca^{2+}, Mg^{2+}, and Na^+, reached their highest concentrations at the
450 bare soil sampling, 8 months after fertilisation (especially for the F_0 treatment). The ion peak found in the bare
451 soil sampling might be attributed to two main factors: i) the interruption of both nutrient uptake by plants, as
452 they were not present since harvest (3·VII), and ion leaching (ceased during a 5-mo period, from the harvest
453 sampling to the bare soil sampling); ii) the release of nutrients from barley belowground biomass
454 decomposition, which in turn, could have induced native soil organic matter mineralisation. Other studies
455 support these assumptions as it is well established that in croplands a maximum of mineral N accumulation
456 and potential leaching occurs after harvest (Harmsen & Schreven, 1955; Macdonald et al., 1989). Furthermore,
457 the intermittent drought simulation conducted in our experiment, which coincided with the post-harvest period,
458 could also have boosted mineralisation (Appel, 1998; Sparling et al., 1995).

459 Remarkably, and as a main research interest of this study, the addition of both rates of fresh biochar
460 significantly reduced NO_3^- concentrations in soil solution at the bare soil sampling compared to its controls

(F_0). Conversely, in the aged biochar scenario none of the ions studied were affected by the biochar treatments. This is partly in agreement with a previous study of our research group using the same biochar, the same biochar application rates, and monitoring the same outdoor mesocosms used for the collection of soil with aged biochar for lysimeters construction. Specifically, a reduced nitrate content in water extracts after 15 months was found for the 50 t ha^{-1} treatment (Marks et al., 2016). But while in the mentioned study the reduction was only found for nitrate, in the present study fresh biochar also provoked a concurrent reduction in soluble Cl^-, Ca^{2+}, $Mg^{2+}$and Na^+ contents, which was more consistent for the F_{12} than for the F_{50} treatment. In contrast, other ions were not significantly affected by any of the biochar treatments at the bare soil sampling (i.e., K^+, SO_4^{2-}, $N\text{-}NO_2^-$ and $N\text{-}NH_4^+$). Previous studies with the same gasification biochar used in this experiment repeatedly reported an increase of K^+ and SO_4^{2-} availability, which was mainly attributed to direct release from biochar over time (Marks et al., 2016; Martos et al., 2020; Ribas et al., 2019). Thus, the increased provision of K^+ and SO_4^{2-} by biochar could have counteracted or diluted the reduction effect seen for these ions. Regarding $N\text{-}NO_2^-$ and $N\text{-}NH_4^+$, the lack of significant changes could be ascribed to its minimal concentrations at the bare soil sampling.

4.2. Nitrate mitigation as affected by fresh biochar addition: appraisal of mechanisms

Several mechanisms behind the nitrate mitigation induced by biochar have been proposed by previous literature and thereafter discussed in this section. The different mechanisms are examined by one or several measurements carried out for this purpose, and grouped as sorption, leaching, microbially-mediated processes, volatilisation, plant uptake, and ecotoxicological effects on key biological groups. Finally, the role of biochar ageing is also explored.

4.2.1. Sorption related mechanisms

One long-accepted mechanism to explain nitrogen retention onto biochar is its capacity to improve soil CEC. Precisely, negatively-charged acid functional groups present in biochar's surface (such as carboxyl or hydroxyl groups similar to those of soil humic acids) are able to electrostatically attract cations such as NH_4^+, preventing them to enter the nitrification pathway (Pal, 2016) or to be easily leached. However, the same biochar used in this experiment was demonstrated to be unable to enhance soil CEC 15 months after its application in outdoor mesocosms in a previous study (Marks et al., 2016). This result was attributed to the high degree of aromaticity

of this gasification biochar, and its concomitant low abundance of surface functional groups as measured by Fourier transform infrared spectroscopy analysis (Marks et al., 2014a). The absence of significant differences in exchangeable ammonium in the biochar treatments at the post-fertilisation sampling in our study further supports this idea, as it was the only sampling with relatively important NH_4^+ concentrations. Another mechanism related to negatively charged biochar surfaces is bridge bonding. NO_3^- retention might occur in biochar by means of polivalent cations, such as Ca^{2+} or Mg^{2+}, acting as bridge bonds between nitrate and the functional groups responsible for CEC (Mukherjee et al., 2011). However, given the lack of differences in KCl and water-extractable N-NO_3^-, and taking into account that NH_4^+ was at minimal concentrations at the bare soil sampling, neither NH_4^+ retention through enhanced CEC nor NO_3^- bridge bonding are regarded as important mechanisms to explain NO_3^- retention at that sampling.

On the other hand, even though biochar is reported to mainly possess a net negative surface charge (Harvey et al., 2012, Novak et al., 2009a), mechanisms for direct NO_3^- retention involving positive charges have also been suggested. Nevertheless, reports of mechanisms of direct NO_3^- sorption, such as biochar's anion exchange capacity (Lawrinenko & Laird, 2015), non-conventional hydrogen bonding (Conte et al., 2014; Fang et al., 2014) or counter-ion displacement (i.e., NO_3^- occupying Cl^- exchange sites) (Fidel et al., 2018) are mainly pH-dependent and favoured in acidic conditions, and therefore not expected in our alkaline soil-biochar system. It has also been suggested that NO_3^- retention on biochar can be due to base functional groups present on biochar's surface pyrolysed at high temperatures (Kameyama al., 2012). However, although the gasification biochar of this study was produced at high temperatures (600-900 ºC), as stated earlier, lack of surface functionality casts doubt on any NO_3^- retention in such functional groups.

Biochar properties able to cause nutrient physical adsorption (physisorption as defined in Rouquerol et al., 2014), such as surface area and porosity, are highly interrelated with surface functionality-mediated retention. Namely, as biochar surface increases, the potential number of functional groups able to adsorb nutrients can also increase, hindering the evaluation of these two mechanisms separately. The biochar in our study presented a relatively low Brunauer–Emmett–Teller (BET) surface area (19.77 $m^2\ g^{-1}$). Instead, total porosity was high (80.6 %), and the pore size distribution showed the following volumes (in $cm^3\ g^{-1}$): macropores = 2.82; mesopores = 0.02; micropores = 0.003 (**Table 1**). The pore volumes values were measured by N_2 sorption and mercury porosimetry, but we lack information about CO_2 adsorption. This latter method enables the

516 characterisation of sub-micropores, covering the smaller range of pores that N_2 sorption doesn't encompass
517 (Brewer et al., 2014). Thus, although we cannot exhaustively describe biochar's porosity, it seems clear that
518 macropores, probably derived from pine-wood cell structures, are the dominant pore size class. Since
519 micropores are the main contributor to the biochar physisorption capacity (Downie et al., 2009), the low
520 volume of micropores and BET surface area lead us to disregard physisorption as an important process in our
521 biochar. On the other hand, macroporosity is relevant to soil hydrology and it is expected that biochars with a
522 high volume of macropores with diameters of greater than 50 nm can have a high degree of water-holding
523 capacity (Joseph et al., 2009). Therefore, the high degree of macroporosity of this biochar is probably behind
524 the higher moisture contents in soil-biochar mixtures at some sampling dates, especially for the F_{50} treatment.
525 It is important to note that at the biochar pore-level not only adsorption can take place but also absorption
526 (Lopez-Capel et al., 2016). In relation to this, Major et al., (2009) stated that biochar porosity can contribute
527 to nutrient sorption through the entrapment of nutrient-containing water within its pores through capillary
528 forces. However, pore-related sorption was discarded to explain the mitigation of NO_3^- in soil solution at the
529 bare soil sampling, since if this mechanism is to be acting, we would expect to have found differences between
530 control and biochar treatments in previous sampling dates.
531 To sum up, both adsorption (via surface functionality bonding and physical means) and nutrient entrapment in
532 biochar pores can be mostly rejected to explain the ionic content decrease at the bare soil sampling.
533 *4.2.2. Leaching*
534 Some authors have reported a decrease in NO_3^- leaching after biochar addition, although explaining this effect
535 through a variety of mechanisms (Ippolito et al., 2012; Jassal et al., 2015; Knowles et al., 2011; Yao et al.,
536 2012). It has been suggested that at biochar application rates >10 t ha^{-1}, which are able to increase available
537 water (Blanco-Canqui, 2017), leaching might be reduced. However, biochar supplementation could also
538 enhance hydraulic conductivity or preferential flow around larger particles resulting in greater leaching and
539 nutrient losses (Clough et al., 2013). For instance, Kameyama et al. (2012) reported that saturated hydraulic
540 conductivity increased when higher rates (≥ 5% w/w) of biochar were applied. In our study, biochar treatments
541 did not cause a significant change in leachate concentrations in any of the studied sampling dates, thus, leaching
542 was not considered as an important escape route in our system that could explain differences in soil solution
543 at the bare soil sampling.
544 *4.2.3. Microbially mediated mechanisms*

545 *4.2.3.1. Organic matter mineralisation vs immobilisation*

546 If mineralisation of residual plant debris and/or soil organic matter was effectively reduced in the fresh biochar
547 treatments in the period from harvest to the bare soil sampling, the observed multiple reduction in ionic content
548 at the bare soil sampling could be explained. Supporting this idea, Marks et al. (2016), in a study using the
549 same biochar and soil as ours, showed that in some of the incubation periods studied, N mineralisation as NO_3^-
550 was reduced for both the 12 and 50 t ha^{-1} biochar treatments after 6 and 12 months of biochar supplementation
551 in soil, with the effect being more pronounced for the 50 t ha^{-1} treatment.

552 However, in our study we lack direct nitrogen mineralisation rates measurements, thus, the mineralisation
553 process is approached as carbon mineralisation rates (Hart et al., 1994; Kätterer & Andrén, 2001), which were
554 measured as CO_2 emission rates using the static chamber methodology and soil basal respiration (BAS). There
555 were no biochar induced differences in BAS or CO_2 chamber-measured emission rates at the bare soil sampling
556 and, indeed, CO_2 chamber-measured emissions were very low in all treatments. By contrast, the CO_2 emission
557 suppression found at the 12th April post-fertilisation sampling for the F_{50} treatment suggests that mineralisation
558 might be reduced (negative priming) at high biochar doses. The cause of CO_2 reduction is out of the scope of
559 this study but possible explanations comprehend not only negative priming (thoroughly reviewed in Whitman
560 et al., 2015) but also mechanisms not related to changes in mineralisation, as direct CO_2 adsorption onto
561 biochar (Madzaki et al., 2016; Sethupathi et al., 2017) or biochar acting as an alkaline trap of CO_2 by promoting
562 its precipitation in the form of carbonates (Fornes et al., 2015). Importantly, even if the negative priming was
563 effectively acting at the post-fertilisation sampling, it could also only have been transitory and did not exert
564 effects at the bare soil sampling. As an example, Naisse et al. (2015), in a study also testing a gasification
565 biochar, reported a negative priming effect that only lasted a few weeks after its application. Furthermore, N
566 and O isotopic composition of nitrate in KCl extracts reinforce this notion as they reveal that both F_0 and F_{50}
567 presented a very similar (not significantly different) δ^{15}N-NO_3 value at the bare soil sampling, which was
568 comprised between the values of soil organic matter and plant debris, hence, indicating a similar extent of
569 mineralisation. Therefore, a possible lowered mineralisation in fresh biochar treatments at the bare soil
570 sampling is not regarded as an important mechanism to explain the differential ion content in soil solution.

571 Regarding a potential role of microbial immobilisation in the last sampling (bare soil) to explain the multiple
572 ion reduction, despite the lack of N_{mic} measurement at that sampling, immobilisation seems an unlikely
573 explanation given that a variety of other ions apart from nitrate were also reduced and not following the known

574 microbial stoichiometry. As an example, Ca^{2+} was reduced ca. 2000 mg kg^{-1} in biochar treatments compared
575 to F_0, while for $N\text{-}NO_3^-$ the difference was of only ca. 300 mg kg^{-1} despite being a macronutrient. Moreover,
576 C_{mic} didn't show differences as a function of biochar treatment at this sampling. As a result, the reduction of
577 ionic content in the fresh biochar treatments as explained by microbial immobilisation is discarded.
578 *4.2.3.2. Nitrification vs denitrification*
579 $N\text{-}NO_3^-$ was the dominant N form in soil solution throughout the entire experiment except for a short period
580 after fertilisation, when $N\text{-}NH_4^+$ gained importance. This pattern is found in most agricultural soils, as
581 nitrification normally converts NH_4^+ into NO_3^- within 2-3 weeks after fertiliser application resulting in NO_3^-
582 accumulation in the soil (Norton, 2008). The rapid onset of nitrification is also supported by isotopic
583 composition analyses of KCl extracts since at the post-fertilisation sampling (5th April) $\delta^{15}N\text{-}NO_3$ slightly
584 decreased with respect to the pre-fertilisation sampling. This is indicative of the nitrification onset given that
585 the generated NO_3^- through nitrification is depleted in $\delta^{15}N$ with respect to the substrate, especially at the
586 beginning of the reaction (Kendall & Aravena, 2000).
587 Although nitrification seems to be a major process in this experimental system, denitrification could also be
588 operating. Therefore, in order to gain insight into whether denitrification was an important process, we
589 examined the N and O isotopic composition of dissolved nitrate, as denitrification has a distinct and predictable
590 effect on $\delta^{15}N\text{-}NO_3$ and $\delta^{18}O\text{-}NO_3$ (Kendall et al., 2008). Namely, denitrification causes a coupled enrichment
591 in $\delta^{15}N\text{-}NO_3$ and $\delta^{18}O\text{-}NO_3$ of the residual nitrate, leading a ratio of isotopic fractionation $\varepsilon^{15}N/\varepsilon^{18}O$ between
592 2:1 and 1:1 depending on the tested conditions (Böttcher et al., 1990; Fukada et al., 2003; Granger et al., 2008;
593 Wunderlich et al., 2013).
594 None of the investigated lysimeters showed a clear denitrification trend except for the F_0 treatment at 7th June
595 and 5th July samplings (both in KCl extracts and leachates) and also for the F_{50} KCl extract at 7th June. However,
596 isotopic composition analyses interpretation is not straightforward since other processes could also have risen
597 $\delta^{15}N\text{-}NO_3$ and $\delta^{18}O\text{-}NO_3$ separately resulting in the same output as denitrification. On the one hand, $\delta^{15}N\text{-}NO_3$
598 could have risen due to the input of $N\text{-}NO_3^-$ derived from nitrification of the highly ^{15}N enriched pig slurry,
599 microbial immobilisation (Kendall et al., 2008) or plant uptake (Craine et al., 2015). On the other hand, $\delta^{18}O\text{-}NO_3$ values could have increased due to a major vapour evaporation in summer months, a process which
601 depletes soil water in the lighter oxygen isotope (Briand et al., 2017) since two atoms of oxygen in NO_3^- are
602 assumed to come from water during nitrification (Hollocher, 1984). Such an effect would be more pronounced

603 in F_0 due to its lower water content (more evaporation expected to have taken place). Despite the uncertainty
604 about the processes that caused δ^{15}N-NO_3 and δ^{18}O-NO_3 enrichment in summer, its punctual occurrence points
605 to denitrification not being an important process. Furthermore, the observed narrow range of δ^{18}O-NO_3
606 underpins this notion (Nikolenko et al., 2018).
607 All things considered, nitrification appears to be the key process in our system, while denitrification would not
608 represent a major force for the nitrate losses observed. In addition, denitrification could not explain the
609 concurrent reduction of the other ionic species besides nitrate.
610 *4.2.4. Ammonia volatilisation*
611 The ammonia volatilisation, assessed shortly after fertilisation, when maximum emissions rates were expected,
612 was not significantly affected by biochar amendment though we found a tendency to higher emission rates in
613 F_{12} treatment. Volatilisation of soil nitrogen as ammonia is promoted in alkaline soils (Rao & Batra 1983), and
614 therefore, biochars with liming capacity might potentially displace the equilibrium between NH_4^+ and NH_3 and
615 promote NH_3 production and volatilisation (Nelissen et al., 2012; Novak et al., 2009b; Taghizadeh-Toosi et al.,
616 2011). However, this is not likely in our soil, since although the biochar was highly alkaline ($pH_{1:20}$ 11.14), it
617 was unable to cause further increases of pH in the already alkaline tested soil ($pH_{1:2.5}$ 8.2) (Marks et al., 2016).
618 We cannot totally discard this mechanism, since we lack ammonia measurements in the samplings after 9 days
619 of the fertilisation event, and mineralisation of barley roots could also have promoted ammonification and
620 hence ammonia volatilisation leading later to lower nitrate levels. However, the lack of significant differences
621 shortly after fertilisation and the fact that volatilisation is unable to explain the concurrent reduction of the
622 other ions seem to discard this mechanism.
623 *4.2.5. Plant nitrogen export*
624 The biochar used in this study has been shown to exert contrasting effects on crop performance. While Marks
625 et al. (2014a) showed an inhibitory effect on barley growth attributed to low P availability (as biochar plausibly
626 promoted its precipitation) in laboratory plant tests, Martos et al. (2020) reported a higher N efficiency uptake
627 but no effects on crop yield in field mesocosms when the same biochar was applied at lower and similar rates
628 in an alkaline soil. Similarly, Marks et al. (2016) revealed no biochar-mediated effects on barley responses the
629 first three years after the application in the same mesocosms where soil with aged biochar was obtained for
630 lysimeters construction, and therefore the same application rate. In agreement with the findings of Martos et

al. (2020) and Marks et al. (2016), in our study nitrogen export was unaffected by biochar treatments, therefore preventing this mechanism as an explanation of the reduced ionic availability at the bare soil sampling.

4.2.6. Ecotoxicological effects on key soil biological groups

Biochar has been proven to contain toxic compounds for microbial communities and other biological groups such as volatile organic compounds, acetaldehyde, aldehydes, and ethylene (Nguyen et al., 2017), conversely, biochar can in turn reduce the bioavailability of toxic chemicals present in soil (Ahmad et al., 2014), so the impact of biochar in soils is hard to predict. The gasification pine-biochar of this study had large quantities of PAH (438 mg kg^{-1}) ten times higher than the maximum values reported for another gasification biochar by Hale et al. (2012), and had a high pH (11.14). Therefore, it has the potential to provoke toxic impacts to soil organisms. However, we failed to find any effect on collembolans or algae performance, nor in N-cycle functional microbial groups. This is in agreement with previous laboratory studies using the same fresh gasification biochar, that failed to find negative effects on collembolans at a higher concentration than the ones on this experiment (considering that the 50 t ha^{-1} application approximately corresponds to a 0.38% w/w), but with effects on enchytraeids at relatively close concentrations (Marks et al., 2014b), and mainly attributed to the increasing pH with increasing dose, something that was not found in our study. However, this biochar was shown to decrease faunal feeding activities the three years after biochar addition in the soil mesocosms where the soil with aged biochar was collected (Marks et al. 2016) without any detectable increase in soil pH, but we did not found this effect after six years in the same plots (unpublished results).

Regarding N-cycle microbial groups, biochar has been linked to nitrification inhibition of the nitrifier *Nitrosomonas* by the release of α-pinene in a pine-derived biochar similar to ours (Clough et al., 2010). In addition, since PAH can exert toxic effects on nitrifiers and denitrifiers (Guo et al., 2011; Sverdrup et al., 2002) some inhibiting effects could be expected in this biochar with high values of this compound. However, microbial functional diversity of N-cycle microorganisms at 12th April sampling did not show significant effects of biochar either when measured as gene copies or transcripts. Although a slight non-significant reduction in nitrifiers was noted for the F_{12} treatment, any ecotoxicological effect seems unlikely because a similar or higher reduction could be expected in F_{50}. In summary, and despite the high PAH load and pH value of this biochar, ecotoxicological effects on N cycling via soil organisms seem to be limited.

4.2.7 *On the potential role of ageing: is biochar pore occlusion by organo-mineral layers behind the reduction of soil nitrate?*

As biochar ages in soil, fragmentation and changes on the surface of biochar particles including redox reactions, solubilisation and interactions with microbes and organic matter, can alter its properties, which can, in turn, influence biochar effects on soil properties (Blanco-Canqui, 2017; Joseph et al., 2010). Namely, it has been recurrently claimed that CEC increases with biochar ageing through oxidative reactions on biochar surfaces as well as through sorption of organic matter, both processes leading to an increase in surface functionality (Kookana et al., 2011; Liang et al., 2006). By contrast, Hagemann et al. (2017) proposed that the main mechanism involved in biochar ageing is not surface oxidation but the formation of an organo-mineral coating which has been proved in co-composted biochar (Kammann et al., 2015) but also in soil-aged biochar. This could have a collateral consequence, which is the occlusion of nutrient-loaded water within pores, first retained by capillarity forces, and then trapped due to the organo-mineral plaque obstructing the pore (Joseph et al., 2018). Importantly, other studies of soil aged biochar particles have also reported the formation of porous agglomerates on the surfaces of the biochar, which in some cases implied the formation of organo-mineral associations (Archanjo et al., 2017).

This mechanism could be the one behind the concurrent reduction of nitrates along with other cations and anions in fresh biochar lysimeters in the last sampling of this study, only observed after 8 months of biochar application. Notably, this mechanism could explain why in other studies some biochar effects upon nutrient availability are only found long after its application. As an example, Ventura et al. (2013) only noted a reduction in NO_3^- leaching after 13-mo of biochar addition. Nevertheless, the formation of organo-mineral coatings in soil-aged biochar particles cited in the study of Hagemann et al. (2017) had been described after 2.5 years of ageing in soil. By contrast, in our study, the reduced ionic content was observed in a shorter timeframe, so it is difficult to ascertain whether this time period is sufficient for this occlusion to occur. Some examples concerning the timing of the process in field aged biochar include Lin et al. (2012), that revealed that soil mineral phases attachment onto the biochar surfaces occurred within the first year (c.a. 4 months) of incubation, while Mukherjee et al. (2014) observed the formation of organic matter coatings within 15 months of biochar ageing, and de la Rosa et al. (2018) reported coatings of soil organic matter and microbial mats onto biochar after 24 months.

In the study of Joseph et al. (2018), it is also hypothesised that the concentration gradient emerging from drying in the composting process could boost ion movement into biochar pores (which are subsequently trapped in the pores), therefore it is plausible that our drought simulation exerted a similar effect. By contrast, a possible

689 drawback for the organo-mineral coating mechanism explanation in our system might be the lack of a linear
690 effect of biochar addition in ionic reduction since the effect is more apparent in F_{12} than in F_{50}. However, this
691 might be explained by the findings of Teixidó et al. (2013), who found a larger loss of biochar surface area in
692 the 1% than in the 2% biochar-soil mixtures after an artificial ageing process. This effect was attributed to a
693 better foulant coverage of organic matter when biochar is more diluted in soil. In this regard, differential
694 organic matter fouling and/or microbial colonisation could explain the lack of linearity in this study.
695 The organo-mineral coating hypothesis might also explain the general lack of significant results in the biochar
696 aged scenario, since once biochar pores are occluded, its capacity to interact with water, nutrients and
697 microorganisms might be limited (Mukherjee et al., 2011). For instance, the lack of moisture content
698 enhancement in the aged biochar scenario is consistent with pore clogging, as observed by Sorrenti et al.
699 (2016).
700 Our results highlight the importance of long-term studies to validate the observed biochar effects in the short-
701 term, which is mandatory considering biochar long residence time in soil, in order to prevent contrary or
702 unintended effects than the ones motivating their use in soil as a result of ageing processes. The ageing
703 mechanism indicated in this study, suggested as plausible by default of other mechanisms, has been only
704 recently reported in the literature and require further research for its validation. Nanoscale analysis of biochar
705 surfaces by means of microscopy and spectroscopic techniques is therefore needed to gain further insight onto
706 biochar evolution over time and specifically on organo-mineral coating formation.
707

708 **5. Conclusions**

709 As expected by previous research with the same pine gasification biochar, a significant decrease of nitrate in
710 soil solution was confirmed. However, this result was only true for the fresh biochar scenario and not for the
711 aged one. In the present study, both biochar application rates (12 and 50 t ha^{-1}) in the fresh biochar scenario
712 reduced nitrate levels as well as other ions (chloride, sodium, magnesium and calcium) at the bare soil
713 sampling, the effect being more apparent for the 12 t ha^{-1} treatment. However, the ionic content reduction was
714 only found for soil solution and not in leachates, therefore, bringing into question biochar's ability to mitigate
715 nitrate aquifer pollution.

716 Sorption, leaching, microbial mineralisation and immobilisation, ammonia volatilisation, plant export, and
717 ecotoxicological effects on biological groups regulating N-cycle were discarded as explanatory mechanisms
718 for the observed ionic content reduction. Notably, this reduction was only detected after 8 months of biochar
719 application, presumably indicating the need for biochar to be in contact with soil in order to provoke effects.
720 By contrast, in the aged biochar scenario, after 6 years of contact with soil, no effects were found. In this sense,
721 the formation of an organo-mineral coating trapping nutrient-rich water could explain the punctual and
722 concurrent reduction of the different ionic species in the fresh biochar scenario but may also be the cause of
723 the lack of effects in the aged biochar scenario, since once the pores are clogged by this coating its retentive
724 properties could be lost. Nevertheless, our data does not allow us to demonstrate this mechanism and thus more
725 studies are needed to support this hypothesis.

726

727 **Acknowledgments**

728 This work was funded by the project FERTICHAR (AGL2015-70393-R) of the Spanish Ministry of Economy
729 and Competitiveness and partly by the projects PACE-ISOTEC (CGL2017-87216-C4-1-R) financed by the
730 Spanish Government and AEI/FEDER from the UE and MAG (2017-SGR-1733), financed by the Catalan
731 Government.

732

733 **References**

734 Ahmad, M., Rajapaksha, A. U., Lim, J. E., Zhang, M., Bolan, N., Mohan, D., Vithanage, M., Lee, S. S., & Ok,
735 Y. S. (2014). Biochar as a sorbent for contaminant management in soil and water: a review. *Chemosphere,*
736 *99*, 19–33. doi:10.1016/j.chemosphere.2013.10.071.

737 Appel, T. (1998). Non-biomass soil organic N—the substrate for N mineralization flushes following soil
738 drying–rewetting and for organic N rendered $CaCl_2$-extractable upon soil drying. *Soil Biology and*
739 *Biochemistry, 30*(10-11), 1445-1456. https://doi.org/10.1016/S0038-0717(97)00230-7

740 Archanjo, B.S., Mendoza, M.E., Albu, M., Mitchell, D.R.G., Hagemann, N., Mayrhofer, C., Mai, T.L.A.,Weng,
741 Z., Kappler, A., Behrens, S., Munroe, P., Achete, C.A., Donne, S., Araujo, J.R., van Zwieten, L., Horvat,
742 J., Enders, A., & Joseph, S. (2017). Nanoscale analyses of the surface structure and composition of
743 biochars extracted from field trials or after co-composting using advanced analytical electron microscopy.
744 *Geoderma*, *294*, 70–79. https://doi.org/10.1016/j.geoderma.2017.01.037

745 Asada, T., Ohkubo, T., Kawata, K., & Oikawa, K. (2006). Ammonia adsorption on bamboo charcoal with acid
746 treatment. *Journal of Health Science*, *52*(5), 585–589. https://doi.org/10.1248/jhs.52.585

747 Barton, L., Kiese, R., Gatter, D., Butterbach-Bahl, K., Buck, R., Hinz, C., & Murphy, D. V. (2008). Nitrous
748 oxide emissions from a cropped soil in a semi-arid climate. Global Change Biology, *14*(1), 177-192.
749 https://doi.org/10.1111/j.1365-2486.2007.01474.x

750 Blanco-Canqui, H. (2017). Biochar and soil physical properties. *Soil Science Society of America Journal*,
751 *81*(4), 687–711. https://doi.org/10.2136/sssaj2017.01.0017

752 Böttcher, J., Strebel, O., Voerkelius, S., & Schmidt, H.-L. (1990). Using isotope fractionation of nitrate-
753 nitrogen and nitrate-oxygen for evaluation of microbial denitrification in a sandy aquifer. *Journal of*
754 *Hydrology, 114*(3–4), 413–424. https://doi.org/10.1016/0022-1694(90)90068-9

755 Bouwman, A.F. (1990). Exchange of greenhouse gases between terrestrial ecosystems and the atmosphere. In:
756 Bouwman, A.F. (Ed.). Soils and the greenhouse effect. Chichester: John Wiley & Sons Ltd. (pp. 61–127)

757 Bremner, J. M. (1965). Total nitrogen. In: Black, C. A. (Ed.). Methods of soil analysis Part 2. Number *9* in
758 series Agronomy. *American Society of Agronomy, Inc*. Publisher Madisson, Wilconsin, USA. (pp. 1103–
759 1105) http://doi.org/10.2134/agronmonogr9.2.c32

760 Bremner, J.M., & Mulvaney, C.S. (1983) Nitrogen-Total. In: Page, A.L., (Ed.), Methods of Soil Analysis. Part
761 2. Chemical and Microbiological Properties, American Society of Agronomy, Soil Science Society
762 of America. (pp. 595–624) http://doi.org/10.2134/agronmonogr9.2.2ed.c31

763 Brewer, C. E., Chuang, V. J., Masiello, C. A., Gonnermann, H., Gao, X., Dugan, B., Driver, L.E., Panzacchi,
764 P., Zygourakis, Z., & Davies, C. A. (2014). New approaches to measuring biochar density and porosity.
765 *Biomass and Bioenergy*, *66*, 176–185. https://doi.org/10.1016/j.biombioe.2014.03.059

766 Briand, C., Sebilo, M., Louvat, P., Chesnot, T., Vaury, V., Schneider, M., & Plagnes, V. (2017). Legacy of
767 contaminant N sources to the NO_3^- signature in rivers: A combined isotopic (δ^{15}N-NO_3^-, δ^{18}O-NO_3^-, δ^{11}B)
768 and microbiological investigation. *Scientific Reports*, 7, 41703. https://doi.org/10.1038/srep41703

769 Brookes, P.C., & Joergensen, R.G., (2006) Microbial biomass measurements by fumigation- extraction. In:
770 Bloem, J., Hopkins, D.W., Benedetti, A. (Eds.), Microbial Methods for Assessing Soil Quality. CABI
771 Publishing, King's Lynn. (pp. 77–83) http://doi.org/10.1079/9780851990989.0077

772 Cabrera, M. L., & Beare, M. H. (1993). Alkaline persulfate oxidation for determining total nitrogen in
773 microbial biomass extracts. *Soil Science Society of America Journal*, *57*(4), 1007–1012.
774 https://doi.org/10.2136/sssaj1993.03615995005700040021x

775 Cameron, K. C., Di, H. J., & Moir, J. L. (2013). Nitrogen losses from the soil/plant system: A review. *Annals*
776 *of Applied Biology, 162(2),* 145–173. https://doi.org/10.1111/aab.12014

777 Clough, T. J., Bertram, J. E., Ray, J. L., Condron, L. M., O'Callaghan, M., Sherlock, R. R., & Wells, N. S.
778 (2010). Unweathered wood biochar impact on nitrous oxide emissions from a bovine-urine-amended
779 pasture soil. *Soil Science Society of America Journal*, *74*(3), 852–860.
780 https://doi.org/10.2136/sssaj2009.0185

781 Clough, T. J., Condron, L. M., Kammann, C., & Müller, C. (2013). A Review of Biochar and Soil Nitrogen
782 Dynamics. *Agronomy*, *3*, 275–293. https://doi.org/10.3390/agronomy3020275

783 Collier, S. M., Ruark, M. D., Oates, L. G., Jokela, W. E., & Dell, C. J. (2014). Measurement of greenhouse gas
784 flux from agricultural soils using static chambers. *JoVE (Journal of Visualized Experiments), 90*, e52110.
785 https://doi:10.3791/52110

786 Conte, P., Hanke, U. M., Marsala, V., Cimoò, G., Alonzo, G., & Glaser, B. (2014). Mechanisms of water
787 interaction with pore systems of hydrochar and pyrochar from poplar forestry waste. *Journal of*
788 *Agricultural and Food Chemistry*, *62*(21), 4917–4923. https://doi.org/10.1021/jf5010034

789 Coplen, T. B. (2011). Guidelines and recommended terms for expression of stable-isotope-ratio and gas-ratio
790 measurement results. *Rapid communications in mass spectrometry*, *25*(17), 2538–2560.
791 https://doi.org/10.1002/rcm.5129

792 Craine, J.M., Brookshire, E.N.J., Cramer, M.D., Hasselquist, N.J., Koba, K., Marin-Spiotta, E., & Wang, L.,
793 (2015). Ecological interpretations of nitrogen isotope ratios of terrestrial plants and soils. *Plant and Soil,*
794 *396*, 1–26. https://doi.org/10.1007/s11104-015-2542-1

795 Davidson, E. A., David, M. B., Galloway, J. N., Goodale, C. L., Haeuber, R., Harrison, J. A., *Howarth, R.W.,*
796 *Jaynes, D.B., Lowrance, R.R., Thomas, N.B., Peel, J.L., Pinder, R.W., Porter, E., Snyder, C.S., Townsend,*
797 *A.R., & Ward, M.H.* (2011). Excess nitrogen in the US environment: trends, risks, and solutions. *Issues*
798 *in Ecology*, (15).

799 De Klein, C. & Harvey, M. (2015). Nitrous oxide chamber methodology guidelines, Ministry for Primary
800 Industries: Wellington, New Zealand.

801 De la Rosa, J. M., Rosado, M., Paneque, M., Miller, A. Z., & Knicker, H. (2018). Effects of aging under field
802 conditions on biochar structure and composition: Implications for biochar stability in soils. *Science of the*
803 *Total Environment*, *613*, 969-976. https://doi.org/10.1016/j.scitotenv.2017.09.124

804 Dempster, D. N., Jones, D. L., & Murphy, D. V. (2012). Clay and biochar amendments decreased inorganic
805 but not dissolved organic nitrogen leaching in soil. *Soil Research*, *50*(3), 216–221.
806 https://doi.org/10.1071/SR11316

807 DIN 38414-S4. (1984). "German Standard Procedure for Water, Wastewater and Sediment Testing (Group S),"
808 Determination of Leachability by Water, Institutfür Normung, Berlin, Germany.

809 Downie, A., Crosky, A. & Munroe, P. (2009). Physical properties of biochar. In: Lehmann, J., Joseph. S. (Eds.)
810 *Biochar for environmental management: Science and Technology*. Earthscan, London. (pp. 13–32)

811 Doydora, S.A., Cabrera, M.L., Das, K.C., Gaskin, J.W., Sonon, L.S., & Miller, W.P. (2011). Release of nitrogen
812 and phosphorus from poultry litter amended with acidified biochar. *International Journal of*
813 *Environmental Research and Public Health*, *8*(5), 1491–1502. https://doi.org/10.3390/ijerph8051491

814 Fang, Q., Chen, B., Lin, Y., & Guan, Y. (2014). Aromatic and hydrophobic surfaces of wood-derived biochar
815 enhance perchlorate adsorption via hydrogen bonding to oxygen-containing organic groups.
816 *Environmental science & technology, 48* (1), 279–288. https://doi:10.1021/es403711y

817 Fidel, R. B., Laird, D. A., & Spokas, K. A. (2018). Sorption of ammonium and nitrate to biochars is electrostatic
818 and pH-dependent. *Scientific Reports*, *8*(1), 1–10. https://doi.org/10.1038/s41598-018-35534-w

819 Fornes, F., Belda, R. M., & Lidón, A. (2015). Analysis of two biochars and one hydrochar from different
820 feedstock: focus set on environmental, nutritional and horticultural considerations. *Journal of Cleaner*
821 *Production*, *86*, 40–48. https://doi.org/10.1016/j.jclepro.2014.08.057

822 Fukada, T., Hiscock, K. M., Dennis, P. F., & Grischek, T. (2003). A dual isotope approach to identify
823 denitrification in groundwater at a river-bank infiltration site. *Water Research*, *37*(13), 3070–3078.
824 https://doi.org/10.1016/S0043-1354(03)00176-3

825 Galloway, J. N., Aber, J. D., Erisman, J. W., Seitzinger, S. P., Howarth, R. W., Cowling, E. B., & Cosby, B. J.
826 (2003). The nitrogen cascade. *Bioscience*, *53*(4), 341–356. https://doi.org/10.1641/0006-
827 3568(2003)053[0341:TNC]2.0.CO;2

828 Glaser, B., Schmidt, H-P., & Shackley, S. (2016). Introduction. In: Shackley, S., Ruysschaert, G., Zwart, K., &
829 Glaser, B. (Eds.). *Biochar in European Soils and Agriculture*. Routledge. (pp. 1–17)
830 https://doi.org/10.4324/9781315884462

831 Granger, J., Sigman, D.M., Lehmann, M.F., & Tortell, P.D. (2008). Nitrogen and oxygen isotope fractionation
832 during dissimilatory nitrate reduction by denitrifying bacteria. *Limnology and Oceanography, 53*, 2533–
833 2545. https://doi.org/10.4319/lo.2008.53.6.2533

834 Griffiths, R. I., Whiteley, A. S., O'Donnell, A. G., & Bailey, M. J. (2000). Rapid method for coextraction of
835 DNA and RNA from natural environments for analysis of ribosomal DNA-and rRNA-based microbial
836 community composition. *Applied and Environmental Microbiology*, *66*(12), 5488–5491.
837 https://doi.org/10.1128/AEM.66.12.5488-5491.2000

838 Guo, G., Deng, H., Qiao, M., Mu, Y., & Zhu, Y. (2011). Effect of pyrene on denitrification activity and
839 abundance and composition of denitrifying community in an agricultural soil. *Environmental Pollution*,
840 *159*(7), 1886–1895. https://doi.org/10.1016/j.envpol.2011.03.035

841 Hagemann, N., Harter, J., & Behrens, S. (2016). Elucidating the Impacts of Biochar Applications on Nitrogen
842 Cycling Microbial Communities. In *Biochar Application: Essential Soil Microbial Ecology*. Elsevier Inc.
843 (pp. 163–198) http://doi.org/10.1016/B978-0-12-803433-0.00007-2

844 Hagemann, N., Joseph, S., Schmidt, H. P., Kammann, C. I., Harter, J., Borch, T., Young, R.B.,Varga, K.,
845 Taherymoosavi, S., Elliott, W., McKenna, A., Albu, M., Mayrhofer, C., Obst, M., Conte, P., Dieguez-
846 Alonso, A., Orsetti, S., Subdiaga, E., Behrens, S., & Kappler, A. (2017). Organic coating on biochar
847 explains its nutrient retention and stimulation of soil fertility. *Nature Communications*, *8*(1).
848 https://doi.org/10.1038/s41467-017-01123-0

849 Hale, S. E., Lehmann, J., Rutherford, D., Zimmerman, A. R., Bachmann, R. T., Shitumbanuma, V., O'Toole,
850 A., Sundqvist, K.L., Arp, H.P.H., & Cornelissen, G. (2012). Quantifying the total and bioavailable
851 polycyclic aromatic hydrocarbons and dioxins in biochars. *Environmental Science and Technology*,
852 *46*(5), 2830–2838. https://doi.org/10.1021/es203984k

853 Harmsen, G. W., & Van Schreven, D. A. (1955). Mineralization of organic nitrogen in soil. *Advances in*
854 *agronomy*, *7*, 299-398. http://doi.org/10.1016/S0065-2113(08)60341-7

855 Hart, S. C., Nason, G. E., Myrold, D. D., & Perry, D. A. (1994). Dynamics of gross nitrogen transformations
856 in an old‐growth forest: The carbon connection. *Ecology, 75*(4), 880-891.
857 http://doi.org/10.2307/1939413

858 Harter, J., Krause, H.M., Schuettler, S., Ruser, R., Fromme, M., Scholten, T., Kappler, A., & Behrens, S. (2014).
859 Linking N_2O emissions from biochar-amended soil to the structure and function of the N-cycling
860 microbial community. *ISME Journal, 8*, 660–674. https://doi.org/10.1038/ismej.2013.160

861 Harvey, O. R., Herbert, B. E., Kuo, L. J., & Louchouarn, P. (2012). Generalized two-dimensional perturbation
862 correlation infrared spectroscopy reveals mechanisms for the development of surface charge and
863 recalcitrance in plant-derived biochars. *Environmental science & technology*, *46*(19), 10641–10650.
864 https://doi.org/10.1021/es302971d

865 Hedqvist, H., & Udén, P. (2006). Measurement of soluble protein degradation in the rumen. *Animal feed*
866 *science and technology, 126* (1–2), 1–21. https://doi:10.1016/j.anifeedsci.2005.05.011

867 Hollocher, T. C. (1984). Source of the oxygen atoms of nitrate in the oxidation of nitrite by *Nitrobacter agilis*
868 and evidence against a PON anhydride mechanism in oxidative phosphorylation. *Archives of*
869 *Biochemistry and Biophysics*, *233*(2), 721–727. https://doi.org/10.1016/0003-9861(84)90499-5

IPCC, 2014: *Climate Change 2014: Synthesis Report. Contribution of Working Groups I, II and III to the Fifth Assessment Report of the Intergovernmental Panel on Climate Change* [Core Writing Team, R.K. Pachauri and L.A. Meyer (Eds.)]. IPCC, Geneva, Switzerland, 151 pp.

Ippolito, J. A., Novak, J. M., Busscher, W. J., Ahmedna, M., Rehrah, D., & Watts, D. W. (2012). Switchgrass Biochar Affects Two Aridisols. *Journal of Environmental Quality*, *41*(4), 1123–1130. https://doi.org/10.2134/jeq2011.0100

ISO 11267. (1999). Soil quality - Inhibition of reproduction of Collembola (*Folsomia candida*) by soil pollutants.

ISO 23470. (2007). Soil quality - Determination of effective cation exchange capacity (CEC) and exchangeable cations using a hexamminecobalt trichloride solution.

ISO/TS 14256-1. (2003). Soil quality -determination of nitrate, nitrite and ammonium in field – moist soils by extraction with potassium chloride solution – part 1: manual method. NORMSERVIS s.r.o., Czech Republic, pp. 1–14.

Jassal, R. S., Johnson, M. S., Molodovskaya, M., Black, T. A., Jollymore, A., & Sveinson, K. (2015). Nitrogen enrichment potential of biochar in relation to pyrolysis temperature and feedstock quality. *Journal of Environmental Management*, *152*, 140–144. https://doi.org/10.1016/j.jenvman.2015.01.021

Joseph, S., Peacocke, C., Lehmann, J., & Munroe, P. (2009). Developing a biochar classification and test methods. In: Lehmann, J., Joseph. S. (Eds.) *Biochar for environmental management: Science and Technology*. Earthscan, London. (pp. 107–126)

Joseph, S.D., Camps-Arbestain, M., Lin, Y., Munroe, P., Chia, C.H., Hook, J., Van Zwieten, L., Kimber, S., Cowie, A., Singh, B.P., Lehmann, J., Foidl, N., Smernik, R.J., & Amonette, J.E. (2010). An investigation into the reactions of biochar in soil. *Australian Journal of Soil Research*, *48*(6–7), 501–515. https://doi.org/10.1071/SR10009

Joseph, S., Kammann, C.I., Shepherd, J.G., Conte, P., Schmidt, H.-P., Hagemann, N., Rich, A.M., Marjo, C.E., Allen, J., Munroe, P., Mitchell, D.R.G., Donne, S., Spokas, K., & Graber, E.R. (2018). Microstructural and associated chemical changes during the composting of a high temperature biochar: Mechanisms for

nitrate, phosphate and other nutrient retention and release. *Science of the Total Environment*, *618*, 1210–1223. https://doi.org/10.1016/j.scitotenv.2017.09.200

Kameyama, K., Miyamoto, T., Shiono, T., & Shinogi, Y. (2012). Influence of Sugarcane Bagasse-derived Biochar Application on Nitrate Leaching in Calcaric Dark Red Soil. *Journal of Environmental Quality*, *41*(4), 1131–1137. https://doi.org/10.2134/jeq2010.0453

Kammann, C.I., Schmidt, H.-P., Messerschmidt, N., Linsel, S., Steffens, D., Müller, C., Koyro, H.-W., Conte, P., & Joseph, S. (2015). Plant growth improvement mediated by nitrate capture in co-composted biochar. *Scientific Reports*, *5*, 1–13. https://doi.org/10.1038/srep11080

Kassambara, A. (2019a). Ggpubr: 'ggplot2' based publication ready plots. https://github.com/kassambara/ggpubr. (accessed 6 June 2020)

Kassambara, A. (2019b). Rstatix: Pipe-friendly framework for basic statistical tests in R. https://github.com/kassambara/rstatix. (accessed 6 June 2020)

Kätterer, T., & Andrén, O. (2001). The ICBM family of analytically solved models of soil carbon, nitrogen and microbial biomass dynamics—descriptions and application examples. *Ecological Modelling, 136*(2-3), 191-207. http://doi.org/10.1016/S0304-3800(00)00420-8

Kendall, C., & Aravena, R. 2000**.** Nitrate isotopes in groundwater systems. In: Cook, P., & Herczeg, A.L. (Eds.), Environmental tracers in subsurface hydrology, Kluwer Academic Publishers, Dordrecht. (pp. 261–297) http://doi.org/10.1007/978-1-4615-4557-6_9

Kendall, C., Elliott, E.M., & Wankel, S.D. 2008. Tracing Anthropogenic Inputs of Nitrogen to Ecosystems. In: Michener, R., & Lajtha, K. (Eds.), Stable Isotopes in Ecology and Environmental Science. Blackwell Publishing Ltd. (pp. 375–449) http://doi.org/10.1002/9780470691854.ch12

Knowles, O. A., Robinson, B. H., Contangelo, A., & Clucas, L. (2011). Biochar for the mitigation of nitrate leaching from soil amended with biosolids. *Science of the total Environment*, *409*(17), 3206-3210. http://doi.org/10.1016/j.scitotenv.2011.05.011

Kookana, R. S., Sarmah, A. K., Van Zwieten, L., Krull, E., & Singh, B. (2011). Biochar application to soil. agronomic and environmental benefits and unintended consequences. *Advances in Agronomy* (1st ed., Vol. 112). Elsevier Inc. (pp. 103–143) https://doi.org/10.1016/B978-0-12-385538-1.00003-2

Lawrinenko, M., & Laird, D. A. (2015). Anion exchange capacity of biochar. *Green Chemistry*, *17*(9), 4628–4636. https://doi.org/10.1039/C5GC00828J

Lehmann, J., da Silva, J. P., Steiner, C., Nehls, T., Zech, W., & Glaser, B. (2003). Nutrient availability and leaching in an archaeological Anthrosol and a Ferralsol of the Central Amazon basin: fertilizer, manure and charcoal amendments. *Plant and Soil*, *249*, 343–357. https://doi.org/10.1023/A:1022833116184

Liang, B., Lehmann, J., Solomon, D., Kinyangi, J., Grossman, J., O'Neill, B., Skjemstad, J.O., Thies, J., Luizao, F.J., Petersen, J., & Neves, E.G. (2006). Black carbon increases cation exchange capacity in soils. *Soil Science Society of America Journal*, *70*(5), 1719–1730. https://doi.org/10.2136/sssaj2005.0383

Lin, Y., Munroe, P., Joseph, S., Kimber, S., & Van Zwieten, L. (2012). Nanoscale organo-mineral reactions of biochars in ferrosol: an investigation using microscopy. *Plant and Soil*, *357*(1–2), 369–380. https://doi.org/10.1007/s11104-012-1169-8

Lopez-Capel, E., Zwart, K., Shackley, S., Postma, R., Stenstrom, J., Rasse, D. P., Budai, A., & Glaser, B. (2016). Biochar properties. In: Shackley, S., Ruysschaert, G., Zwart, K., & Glaser, B. (Eds.). *Biochar in European Soils and Agriculture.* Routledge. (pp. 41-72) https://doi.org/10.4324/9781315884462

Macdonald, A.J., Powlson, D.S., Poulton, P.R. & Jenkinson, D.S. 1989. Unused fertiliser nitrogen in arable soils - Its contribution to nitrate leaching. *Journal of the Science of Food and Agriculture, 46*(4), 407-419. http://doi.org/10.1002/jsfa.2740460404

Madzaki, H., Karimghani, W. A. W. A. B., Nurzalikharebitanim, & Azilbaharialias. (2016). Carbon Dioxide Adsorption on Sawdust Biochar. *Procedia Engineering*, *148*, 718–725. https://doi.org/10.1016/j.proeng.2016.06.591

Major, J., Steiner, C., Downie, A., & Lehmann, J. (2009). Biochar effects on nutrient leaching. In: Lehmann, J., Joseph. S. (Eds.) *Biochar for environmental management: Science and Technology*. Earthscan, London. (pp. 271–288)

946 Mandal, S., Thangarajan, R., Bolan, N. S., Sarkar, B., Khan, N., Ok, Y. S., & Naidu, R. (2016). Biochar-induced
947 concomitant decrease in ammonia volatilization and increase in nitrogen use efficiency by wheat.
948 *Chemosphere*, *142*, 120–127. https://doi.org/10.1016/j.chemosphere.2015.04.086

949 Marks, E. A., Alcañiz, J. M., & Domene, X. (2014a). Unintended effects of biochars on short-term plant growth
950 in a calcareous soil. *Plant and soil*, *385*(1–2), 87–105. https://doi.org/10.1007/s11104-014-2198-2

951 Marks, E. A. N., Mattana, S., Alcañiz, J. M., & Domene, X. (2014b). Biochars provoke diverse soil mesofauna
952 reproductive responses in laboratory bioassays. *European Journal of Soil Biology*, *60*, 104–111.
953 https://doi.org/10.1016/j.ejsobi.2013.12.002

954 Marks, E. A. N., Mattana, S., Alcañiz, J. M., Pérez-Herrero, E., & Domene, X. (2016). Gasifier biochar effects
955 on nutrient availability, organic matter mineralization, and soil fauna activity in a multi-year
956 Mediterranean trial. *Agriculture, Ecosystems and Environment*, *215*, 30–39.
957 https://doi.org/10.1016/j.agee.2015.09.004

958 Martos, S., Mattana, S., Ribas, A., Albanell, E., & Domene, X. (2020). Biochar application as a win-win
959 strategy to mitigate soil nitrate pollution without compromising crop yields: a case study in a
960 Mediterranean calcareous soil. *Journal of Soils and Sediments 20,* 220–233.
961 https://doi.org/10.1007/s11368-019-02400-9

962 Matsumura, S., & Witjaksono, G. (1999). Modification of the Cataldo method for the determination of nitrate
963 in soil extracts by potassium chloride. *Soil Science and Plant Nutrition*, *45*(1), 231–235.
964 https://doi.org/10.1080/00380768.1999.10409338

965 McIlvin, M. R., & Altabet, M. A. (2005). Chemical conversion of nitrate and nitrite to nitrous oxide for nitrogen
966 and oxygen isotopic analysis in freshwater and seawater. *Analytical Chemistry, 77*(17), 5589–5595.
967 https://doi.org/10.1021/ac050528s

968 Mukherjee, A., Zimmerman, A. R., Hamdan, R., & Cooper, W. T. (2014). Physicochemical changes in
969 pyrogenic organic matter (biochar) after 15 months of field aging. *Solid Earth, 5*(2), 693.
970 https://doi.org/10.5194/sed-6-731-2014

971 Mukherjee, A., Zimmerman, A. R., & Harris, W. (2011). Surface chemistry variations among a series of
972 laboratory-produced biochars. *Geoderma*, *163*(3–4), 247–255.
973 https://doi.org/10.1016/j.geoderma.2011.04.021

974 Naisse, C., Girardin, C., Lefevre, R., Pozzi, A., Maas, R., Stark, A., & Rumpel, C. (2015). Effect of physical
975 weathering on the carbon sequestration potential of biochars and hydrochars in soil. *GCB Bioenergy*,
976 *7*(3), 488–496. https://doi.org/10.1111/gcbb.12158

977 Nelissen, V., Rütting, T., Huygens, D., Staelens, J., Ruysschaert, G., & Boeckx, P. (2012). Maize biochars
978 accelerate short-term soil nitrogen dynamics in a loamy sand soil. *Soil Biology and Biochemistry*, *55*, 20–
979 27. https://doi.org/10.1016/j.soilbio.2012.05.019

980 Nelson, D. W., & L. E. Sommers. (1983). Total carbon, organic carbon and organic matter. In: A. L. Page, R.
981 H. Miller & D. R. Keeney, eds., Methods ofsoil analysis, Part 2, ASA Publication No. 9, 2nd ed. American
982 Society of Agronomy Monograph, Madison, WI. (pp. 539–577)
983 http://doi.org/10.2134/agronmonogr9.2.2ed.c29

984 Nguyen, T. T. N., Xu, C. Y., Tahmasbian, I., Che, R., Xu, Z., Zhou, X., Wallace, H.M., & Bai, S. H. (2017,
985 February 15). Effects of biochar on soil available inorganic nitrogen: A review and meta-analysis.
986 *Geoderma 288:*79–96. https://doi.org/10.1016/j.geoderma.2016.11.004

987 Nikolenko, O., Jurado, A., Borges, A. V., Knöller, K., & Brouyère, S. (2018). Isotopic composition of nitrogen
988 species in groundwater under agricultural areas: A review. *Science of the Total Environment, 621*, 1415–
989 1432. https://doi.org/10.1016/j.scitotenv.2017.10.086

990 Norton, J.M. (2008). Nitrification in agricultural soils. In: Schepers, J.S., Raun, W.B., Follett, R.F., Fox, R.H.,
991 & Randall, G.W. (Eds.), Nitrogen in Agricultural Systems. Agronomy Monograph, vol. 49. American
992 Society of Agronomy, Madison, WI. (pp. 173–199) http://doi.org/10.2134/agronmonogr49.c6

993 Novak, J. M., Lima, I., Xing, B., Gaskin, J. W., Steiner, C., Das, K. C., Ahmedna, M., Rehrah, D., Watts, D.W.,
994 Busscher, W.J., & Schomberg, H. (2009a). Characterization of designer biochar produced at different
995 temperatures and their effects on a loamy sand. *Annals of Environmental Science* 3, 195–206.

996 Novak, J. M., Busscher, W. J., Laird, D. L., Ahmedna, M., Watts, D. W., & Niandou, M. A. S. (2009b). Impact
997 of biochar amendment on fertility of a southeastern coastal plain soil. *Soil Science*, *174*(2), 105–112.
998 http://doi.org/10.1097/SS.0b013e3181981d9a

999 OECD (2011), Test No. 201: Freshwater Alga and Cyanobacteria, Growth Inhibition Test, OECD Guidelines
1000 for the Testing of Chemicals, Section 2, OECD Publishing, Paris,
1001 https://doi.org/10.1787/9789264069923-en.

1002 Pal, P. (2016). Biochar effects on greenhouse gas emissions. In: Ok, Y. S., Uchimiya, S. M., Chang, S. X., &
1003 Bolan, N. (Eds.) *Biochar: Production, Characterisation and Applications*. CRC Press. (pp. 360-386)
1004 https://doi.org/10.1201/b18920

1005 Pearson, J., & Stewart, G. R. (1993). The deposition of atmospheric ammonia and its effects on plants. *New*
1006 *phytologist*, *125*(2), 283–305. https://doi.org/10.1111/j.1469-8137.1993.tb03882.x

1007 Pell, M., Stenstrom, J., & Granhall, U. (2006). Soil respiration. In: Bloem, J., Hopkins, D. W., & Benedetti, A.
1008 (Eds.), Microbiological Methods for Assessing Soil Quality. CABI Publishing, King's Lynn.
1009 http://doi.org/10.1079/9780851990989.0117

1010 Powlson, D. S., Addiscott, T. M., Benjamin, N., Cassman, K. G., de Kok, T. M., van Grinsven, H., L'hirondel,
1011 J.L., Avery, A. A., & van Kessel, C. (2008). When Does Nitrate Become a Risk for Humans? *Journal of*
1012 *Environmental Quality*, *37*(2), 291–295. http://doi.org/10.2134/jeq2007.0177

1013 R Core Team (2019). R: A language and environment for statistical computing. R Foundation for Statistical
1014 Computing, Vienna, Austria. URL https://www.R-project.org/. (accessed 24 March 2019)

1015 Rao, D. L. N., & Batra, L. (1983). Ammonia volatilization from applied nitrogen in alkali soils. *Plant and Soil*,
1016 *70*(2), 219–228. https://doi.org/10.1007/BF02374782

1017 Ribas, A., Mattana, S., Llurba, R., Debouk, H., Sebastià, M. T., & Domene, X. (2019). Biochar application and
1018 summer temperatures reduce N_2O and enhance CH_4 emissions in a Mediterranean agroecosystem: Role
1019 of biologically-induced anoxic microsites. *Science of the Total Environment*, *685*, 1075–1086.
1020 https://doi.org/10.1016/j.scitotenv.2019.06.277

Rouquerol, F., Rouquerol, J., Sing, K., Maurin, G., & Llewellyn, P. (2014) .Introduction. In: Rouquerol, F., Rouquerol, J., Sing, K. Adsorption by powders and porous solids: principles, methodology and applications; Academic Press: London, U.K. (pp. 1−24) http://doi.org/10.1016/B978-0-08-097035-6.00001-2

Ryabenko, E., Altabet, M. A., & Wallace, D. W. (2009). Effect of chloride on the chemical conversion of nitrate to nitrous oxide for $\delta^{15}N$ analysis. *Limnology and Oceanography: Methods*, 7 (7), 545–552. https://doi.org/10.4319/lom.2009.7.545

Schomberg H.H., Gaskin J.W., Harris K., Das K.C., Novak J.M., Busscher W.J., Watts D.W., Woodroof R.H., Lima I.M., Ahmedna M., Rehrah D., & Xing B. (2012). Influence of Biochar on Nitrogen Fractions in a Coastal Plain Soil. *Journal of Environmental Quality*, *41*(4), 1087–1095. https://doi.org/10.2134/jeq2011.0133

Sethupathi, S., Zhang, M., Rajapaksha, A. U., Lee, S. R., Nor, N. M., Mohamed, A. R., Al-Wabel, M., Lee, S. S. & Ok, Y. S. (2017). Biochars as potential adsorbers of CH_4, CO_2 and H_2S. *Sustainability (Switzerland)*, *9*(1), 1–10. https://doi.org/10.3390/su9010121

Sohi, S. P., Krull, E., Lopez-Capel, E., & Bol, R. (2010). A review of biochar and its use and function in soil. In: *Advances in agronomy* (Vol. 105, pp. 47–82). Academic Press. http://doi.org/10.1016/S0065-2113(10)05002-9

Soil Survey Staff, (2010). Keys to Soil Taxonomy, 11th ed. USDA—Natural Resources Conservation Service.

Sorrenti, G., Masiello, C. A., Dugan, B., & Toselli, M. (2016). Biochar physico-chemical properties as affected by environmental exposure. *Science of the total Environment*, *563*, 237-246. http://doi.org/10.1016/j.scitotenv.2016.03.245

Sparling, G. P., Murphy, D. V., Thompson, R. B., & Fillery, I. R. P. (1995). Short-term net N mineralization from plant residues and gross and net N mineralization from soil organic-matter after rewetting of a seasonally dry soil. *Soil Research, 33*(6), 961-973. http://doi.org/10.1071/SR9950961

Sverdrup, L. E., Ekelund, F., Krogh, P. H., Nielsen, T., & Johnsen, K. (2002). Soil microbial toxicity of eight polycyclic aromatic compounds : effects on nitrification, the genetic diversity of bacteria, and the total

number of protozoans. *Environmental Toxicology and Chemistry: An International Journal, 21*(8), 1644–1650. https://doi.org/10.1002/etc.5620210815

Taghizadeh‐Toosi, A., Clough, T. J., Condron, L. M., Sherlock, R. R., Anderson, C. R., & Craigie, R. A. (2011). Biochar incorporation into pasture soil suppresses in situ nitrous oxide emissions from ruminant urine patches. *Journal of environmental quality, 40* (2), 468–476. https://doi:10.2134/jeq2010.0419.

Taghizadeh-Toosi, A., Clough, T. J., Sherlock, R. R., & Condron, L. M. (2012). Biochar adsorbed ammonia is bioavailable. *Plant and Soil*, *350*(1–2), 57–69. https://doi.org/10.1007/s11104-011-0870-3

Teixidó, M., Hurtado, C., Pignatello, J. J., Beltrán, J. L., Granados, M., & Peccia, J. (2013). Predicting contaminant adsorption in black carbon (biochar)-amended soil for the veterinary antimicrobial sulfamethazine. *Environmental science & technology*, *47*(12), 6197–6205. https://doi.org/10.1021/es400911c

Töwe, S., Albert, A., Kleineidam, K., Brankatschk, R., Dümig, A., Welzl, G., Munch, J.C., Zeyer, J., & Schloter, M. (2010). Abundance of microbes involved in nitrogen transformation in the rhizosphere of *Leucanthemopsis alpina* (L.) Heywood grown in soils from different sites of the Damma glacier forefield. *Microbial ecology*, *60*(4), 762–770. https://doi.org/10.1007/s00248-010-9695-5

Töwe, S., Wallisch, S., Bannert, A., Fischer, D., Hai, B., Haesler, F., Kleineidam, K., & Schloter, M. (2011). Improved protocol for the simultaneous extraction and column-based separation of DNA and RNA from different soils. *Journal of microbiological methods 84* (3), 406–412. https://doi:10.1016/j.mimet.2010.12.028.

Vance, E.D., Brookes, P.C., & Jenkinson, D.S. (1987). An extraction method for measuring microbial biomass C. *Soil Biology and Biochemistry*, *19*, 697–702. https://doi.org/10.1016/0038-0717(87)90052-6

Ventura, M., Sorrenti, G., Panzacchi, P., George, E., & Tonon, G. (2013). Biochar Reduces Short-Term Nitrate Leaching from A Horizon in an Apple Orchard. *Journal of Environmental Quality*, *42*(1), 76–82. https://doi.org/10.2134/jeq2012.0250

Vitousek, P. M., Aber, J. D., Howarth, R. W., Likens, G. E., Matson, P. A., Schindler, D. W., Schlesinger, W. H., & Tilman, D. G. (1997). Human alteration of the global nitrogen cycle: sources and consequences.

Ecological Applications, 7, 737–750. https://doi.org/10.1890/1051-0761(1997)007[0737:HAOTGN]2.0.CO;2

Voroney, R. P., Brookes, P. C., & Beyaert, R. P. (2008). Soil Microbial Biomass C, N, P, and S. *Soil sampling and methods of analysis*, 2, 637–652. https://doi.org/10.1016/j.soilbio.2015.02.029

Ward, M. H., Jones, R. R., Brender, J. D., de Kok, T. M., Weyer, P. J., Nolan, B. T., Villanueva, C.M., & van Breda, S. G. (2018). Drinking water nitrate and human health: An updated review. *International journal of environmental research and public health, 15*(7), 1557. https://doi.org/10.3390/ijerph15071557

Whitman, T., Singh, B. P., Zimmerman, A. R., Lehmann, J., & Joseph, S. (2015). Priming effects in biochar–amended soils: implications of biochar-soil organic matter interactions for carbon storage. In: Lehmann, J., & Joseph. S. (Eds.) *Biochar for Environmental Management: Science, Technology and Implementation*, *2*. Routledge (pp. 455–488)

Wickham, H. (2016). ggplot2: Elegant Graphics for Data Analysis: Springer-Verlag New York. https://doi.org/10.1007/978-3-319-24277-4

Willis, R. B., Montgomery, M. E., & Allen, P. R. (1996). Improved method for manual, colorimetric determination of total Kjeldhal nitrogen using salicylate. *Journal of Agricultural and Food Chemistry*, *44*(7), 1804–1807. https://doi.org/10.1021/jf950522b

Wunderlich, A., Meckenstock, R.U., & Einsiedl, F. (2013). A mixture of nitrite-oxidizing and denitrifying microorganisms affects the $\delta^{18}O$ of dissolved nitrate during anaerobic microbial denitrification depending on the $\delta^{18}O$ of ambient water. *Geochimica et Cosmochimca Acta, 119*, 31–45. https://doi.org/10.1016/j.gca.2013.05.028

Wyland, L. J., Jackson, L. E., & Brooks, P. D. (1994). Eliminating nitrate interference during Kjeldahl digestion of soil extracts for microbial biomass determination. *Soil Science Society of America Journal*, *58*(2), 357–360. https://doi.org/10.2136/sssaj1994.03615995005800020016x

Yao, Y., Gao, B., Zhang, M., Inyang, M., & Zimmerman, A. R. (2012). Effect of biochar amendment on sorption and leaching of nitrate, ammonium, and phosphate in a sandy soil. *Chemosphere 89*, (11), 1467–1471. doi:10.1016/j.chemosphere.2012.06.002

1100

1101

Parameter	Unit	Value	Method
C	g kg^{-1}	782	elemental analysis
N	g kg^{-1}	2.10	elemental analysis
H	g kg^{-1}	8.81	elemental analysis
S	g kg^{-1}	0.34	elemental analysis
O	g kg^{-1}	70.68	difference of sum of elemental analysis and ash
O/C_{org}		0.10	
H/C_{org}		0.14	
Ash	%	13.61	difference of fixed carbon and volatile matter
Volatile matter	%	2.8	gravimetrically (mass loss between 150ºC-600ºC)
P	g kg^{-1}	1.34	
Na	g kg^{-1}	0.48	
K	g kg^{-1}	9.36	
Ca	g kg^{-1}	20.52	
Mg	g kg^{-1}	2.10	
$CaCO_3$	g kg^{-1}	33.4 ± 0.62	calcimetry
$C\text{-}CO_3$	g kg^{-1}	4 ± 0.62	calcimetry
PAH (16 congeners)	mg kg^{-1}	438	1:1 acetone:hexane extraction, gas chromatography-mass spectrometry
pH (H_2O, 1:20)	-	11.14 ± 0.13	
EC (25ºC, 1:20)	dS m^{-1}	0.3 ± 0.01	
CEC	$mmol_c$ kg^{-1}	3.62 ± 0.11	ISO 23470, 2007
$\delta^{15}N$	‰	-0.9	elemental analysis-isotope ratio mass spectrometry
Surface area (BET)	m^2 g^{-1}	19.77	N_2 adsorption isotherm, 77K
Porosity	%	80.56	Hg porosimetry
Mean porus size	nm	1220.10	Hg porosimetry
Micropore (ø < 2 nm) volume	cm^3 g^{-1}	0.0034	
Mesopore (2 nm ≤ ø ≤ 50 nm) volume	cm^3 g^{-1}	0.0196	
Macropore (ø > 50 nm) volume	cm^3 g^{-1}	2.82	

Table 1. Characteristics of the biochar used in the experiment.

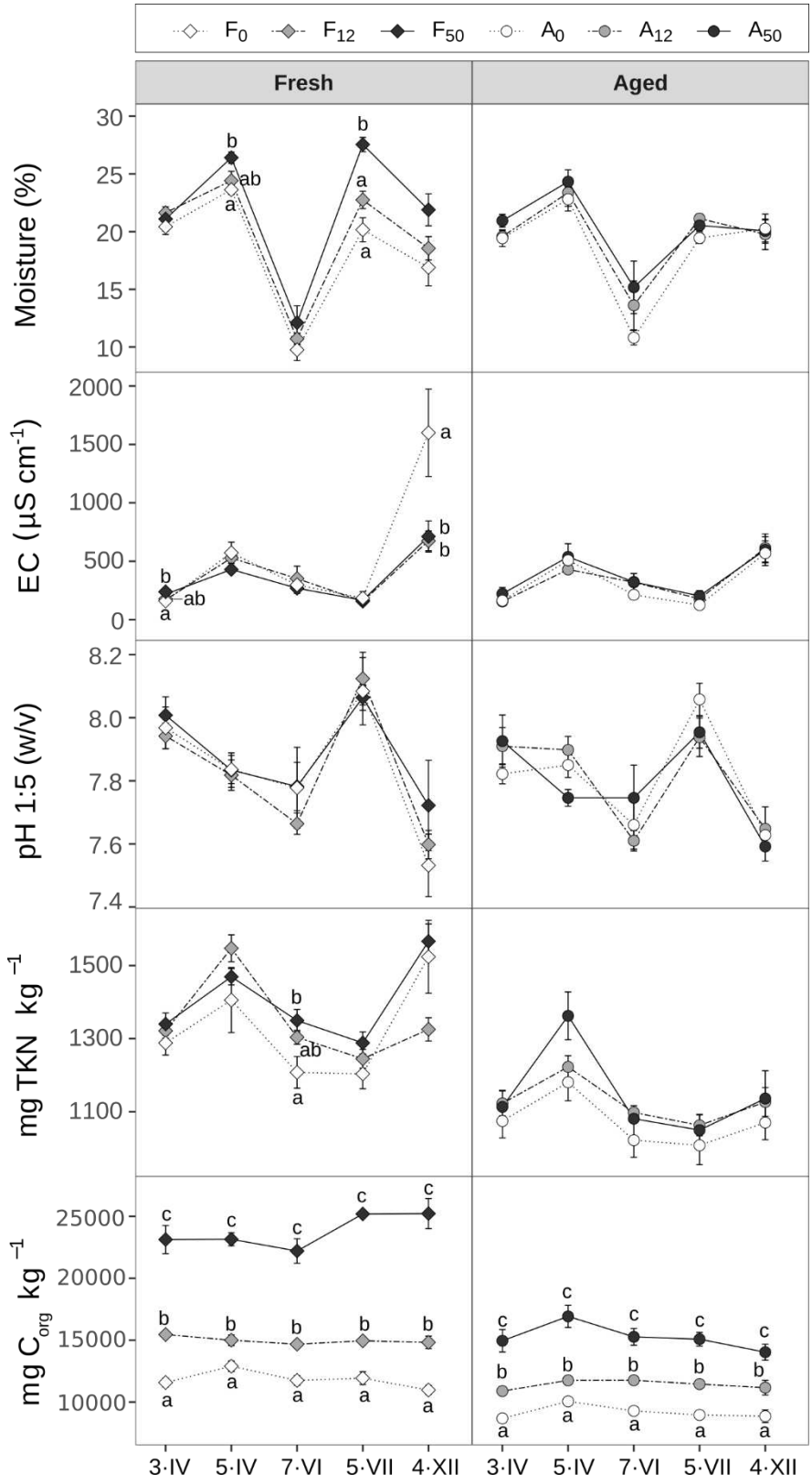

Figure 1. Moisture (%), EC (µS cm^{-1}), pH 1:5 (w/v), Total Kjeldahl Nitrogen (TKN) (mg kg^{-1} DW soil) and C_{org} (mg kg^{-1} DW soil) along five samplings (3·IV = 3rd April; 5·IV = 5th April; 7·VI = 7th June; 5·VII = 5th July and 4·XII = 4th December). Abbreviations for the biochar treatments correspond to: F_0 = fresh 0 t ha^{-1}; F_{12} = fresh 12 t ha^{-1}; F_{50} = fresh 50 t ha^{-1}; A_0 = aged 0 t ha^{-1}; A_{12} = aged 12 t ha^{-1}; A_{50} = aged 50 t ha^{-1}. Symbols represent the mean values, and bars represent the corresponding standard error (n = 5). Different letters indicate statistically significant differences between treatments within a particular sampling.

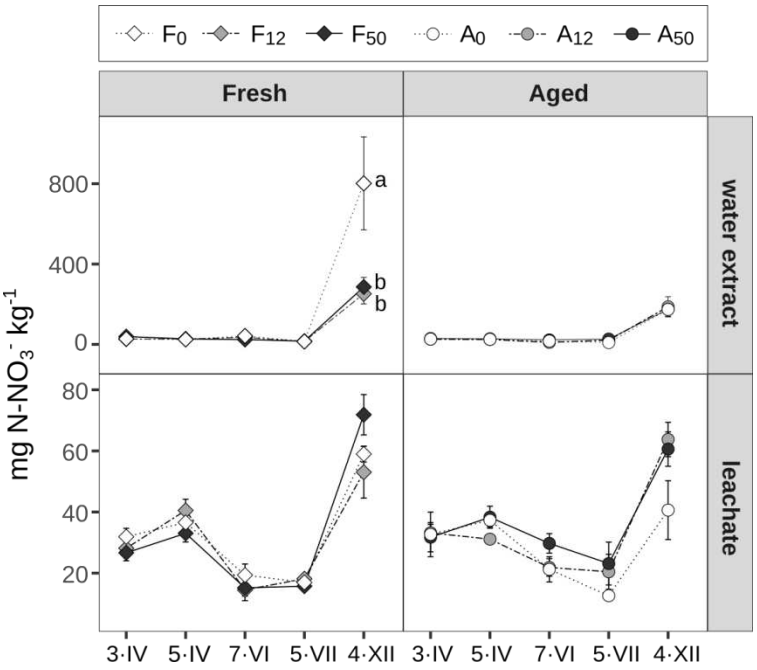

Figure 2. $N\text{-}NO_3^-$ (mg kg^{-1} DW soil) evolution in water extracts (1st row) and leachates (2nd row) along five samplings (3·IV = 3rd April; 5·IV = 5th April; 7·VI = 7th June; 5·VII = 5th July and 4·XII = 4th December). Abbreviations for the biochar treatments correspond to: F_0 = fresh 0 t ha^{-1}; F_{12} = fresh 12 t ha^{-1}; F_{50} = fresh 50 t ha^{-1}; A_0 = aged 0 t ha^{-1}; A_{12} = aged 12 t ha^{-1}; A_{50} = aged 50 t ha^{-1}. Symbols represent the mean values, and bars represent the corresponding standard error (n = 5). Different letters indicate statistically significant differences between treatments within a particular sampling.

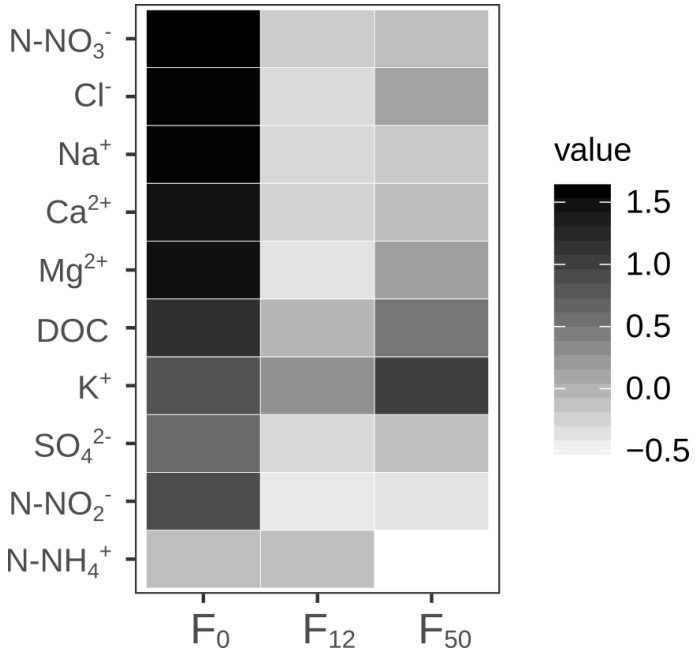

Figure 3. Heatmap of ionic and DOC concentrations in soil solution (mg kg^{-1} DW soil) at the bare soil sampling (4th December) for the fresh biochar scenario. Abbreviations for the biochar treatments correspond to: F_0 = fresh 0 t ha^{-1}; F_{12} = fresh 12 t ha^{-1}; F_{50} = fresh 50 t ha^{-1}; A_0 = aged 0 t ha^{-1}; A_{12} = aged 12 t ha^{-1}; A_{50} = aged 50 t ha^{-1}. The range of values [-0.5 - 1.5] which is used for heatmap colouring refers to standardised variables (mean subtracted and divided by standard deviation) (n = 5).

Parameter	Sampling date	Treatment					
		F_0	**F_{12}**	**F_{50}**	**A_0**	**A_{12}**	**A_{50}**
C_{mic} (mg kg^{-1})	3·IV	357 ± 76.4	398 ± 32.4	358 ± 33.6	243 ± 31.0	261 ± 32.6	202 ± 35.5
	5·IV	337 ± 61.1	355 ± 39.1	423 ± 51.8	207 ± 22.9	268 ± 29.9	182 ± 11.7
	7·VI	275 ± 20.8	271 ± 19.0	278 ± 22.7	150 ± 27.1	205 ± 27.7	216 ± 33.8
	5·VII	277 ± 10.0	263 ± 16.1	240 ± 12.0	191 ± 21.7	183 ± 7.7	173 ± 22.7
	4·XII	291 ± 33.6	273 ± 19.7	255 ± 18.7	199 ± 14.6	225 ± 12.7	238 ± 8.4
N_{mic} (mg kg^{-1})	3·IV	75.1 ± 4.9	89.3 ± 10.3	77.5 ± 3.5	44.3 ± 4.2	53.7 ± 3.6	51.6 ± 3.0
	5·IV	n/a	n/a	n/a	n/a	n/a	n/a
	7·VI	55.4 ± 6.1	66.7 ± 3.4	65.3 ± 6.0	44.6 ± 5.3	46.0 ± 3.9	47.5 ± 5.0
	5·VII	79.5 ± 2.0	80.3 ± 2.2	73.0 ± 3.8	40.3 ± 3.1	47.4 ± 1.4	41.8 ± 2.3
	4·XII	n/a	61.6 ± 3.4	53.5± 11.8	37.4 ± 3.7	34.7 ± 3.3	41.1 ± 4.4
BAS (mg $C\text{-}CO_2$ kg^{-1} h^{-1})	3·IV	0.9 ± 0.0	1.1 ± 0.0	1.1 ± 0.1	0.8 ± 0.1	0.8 ± 0.0	0.8 ± 0.1
	5·IV	0.9 ± 0.1	0.9 ± 0.1	0.9 ± 0.0	0.8 ± 0.1	0.7 ± 0.0	0.9 ± 0.1
	7·VI	0.8 ± 0.0	0.7 ± 0.1	0.9 ± 0.1	0.7 ± 0.0 **a**	0.9 ± 0.1 **ab**	1.0 ± 0.1 **b**
	5·VII	0.7 ± 0.1	0.8 ± 0.1	1.0 ± 0.0	0.5 ± 0.1	0.6 ± 0.0	0.5 ± 0.1
	4·XII	0.6 ± 0.1	0.9 ± 0.1	0.8 ± 0.1	0.5 ± 0.1	0.7 ± 0.1	0.6 ± 0.1

Table 2. Average values of C_{mic}, N_{mic} (mg kg^{-1} DW soil) and BAS (mg $C\text{-}CO_2$ kg^{-1} h^{-1}) per treatment ± standard errors (n = 5) along five sampling dates (3·IV = 3rd April; 5·IV = 5th April; 7·VI = 7th June; 5·VII = 5th July and 4·XII = 4th December). Abbreviations for the biochar treatments correspond to: F_0 = fresh 0 t ha^{-1}; F_{12} = fresh 12 t ha^{-1}; F_{50} = fresh 50 t ha^{-1}; A_0 = aged 0 t ha^{-1}; A_{12} = aged 12 t ha^{-1}; A_{50} = aged 50 t ha^{-1}. Letters in bold indicate significant differences between treatments for a specific sampling date and n/a = not available.

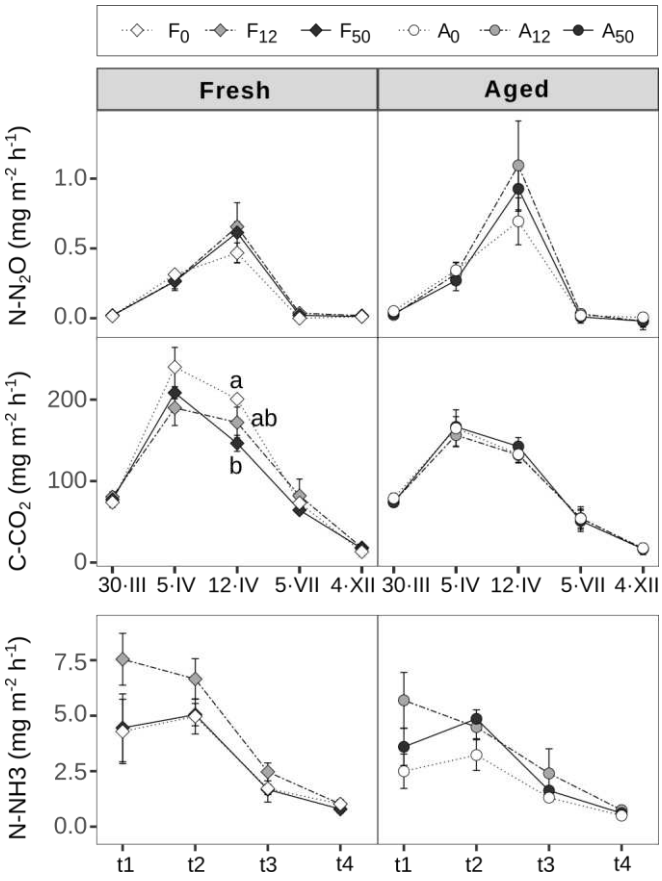

Figure 4. Emission rates of N-N_2O, C-CO_2, and N-NH_3 (mg m^{-2} h^{-1}). Abbreviations for the biochar treatments correspond to: F_0 = fresh 0 t ha^{-1}; F_{12} = fresh 12 t ha^{-1}; F_{50} = fresh 50 t ha^{-1}; A_0 = aged 0 t ha^{-1}; A_{12} = aged 12 t ha^{-1}; A_{50} = aged 50 t ha^{-1}. Different letters indicate statistically significant differences between treatments within a particular sampling. N-N_2O and C-CO_2 were measured along five different samplings (30·III = 30th March; 5·IV = 5th April; 12·IV = 12th April; 5·VII = 5th July and 4·XII = 4th December), symbols represent the mean values, and bars represent the corresponding standard error, n is ≤ 5 as values were filtered (see 2.4 section in methodology). N-NH_3 was measured along 4 sampling periods after the fertilisation with pig slurry (**t1** = 3/4/17-5/4/17; **t2** = 5/4/17-6/4/17; **t3** = 6/4/17-7/4/17; **t4** = 10/4/17-12/4/17), symbols represent the mean values, and bars represent the corresponding standard error (n = 5).

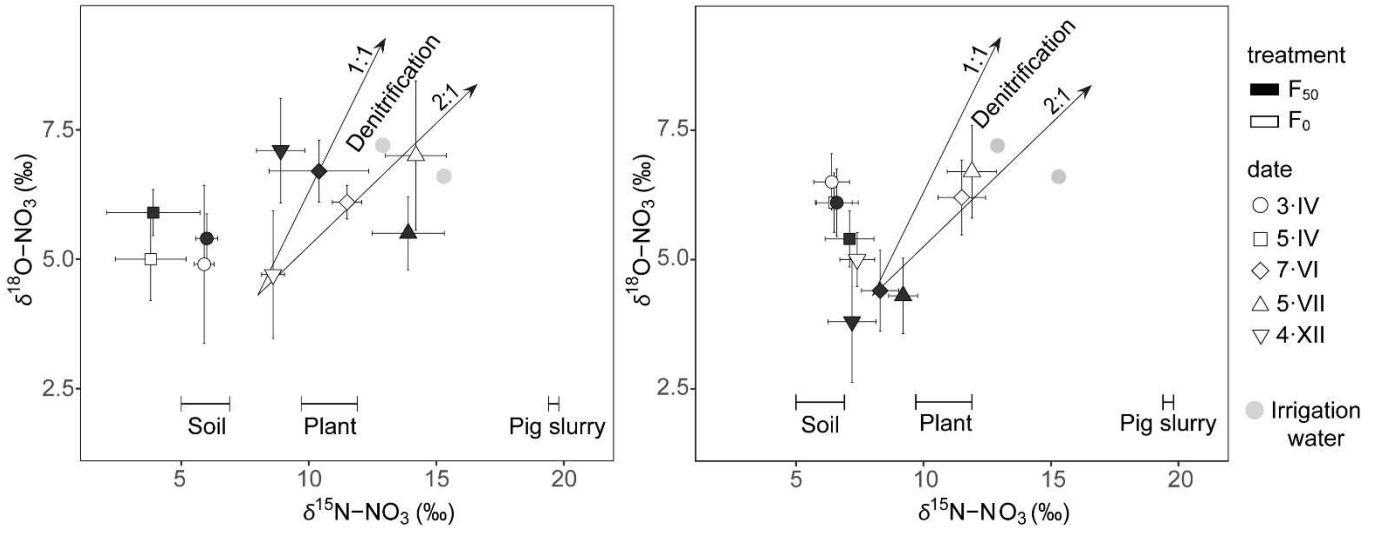

Figure 5. $\delta^{18}O$ and $\delta^{15}N$ of nitrate measured in KCl extracts (left graph) and leachates (right) for the fresh biochar scenario along five different samplings (3·IV = 3rd April; 5·IV = 5th April; 7·VI = 7th June; 5·VII = 5th July and 4·XII = 4th December). Symbols with error bars represent the mean values and standard error (n = 5) respectively. The two arrows indicate typical expected slopes for values resulting from denitrification. Abbreviations for the biochar treatments correspond to: F_0 = fresh 0 t ha^{-1}; F_{50} = fresh 50 t ha^{-1}. $\delta^{15}N$ of soil, harvested plants and pig slurry, and also $\delta^{15}N$ vs $\delta^{18}O$ of dissolved NO_3^- from irrigation water are shown.

Parameter	Treatment					
	F_0	**F_{12}**	**F_{50}**	**A_0**	**A_{12}**	**A_{50}**
Straw weight (g)	14.0 ± 0.8	14.8 ± 0.5	15.0 ± 0.8	12.7 ± 0.3	10.1 ± 1.7	7.4 ± 2.8
Grain weight (g)	6.2 ± 0.9	6.5 ± 0.6	7.4 ± 0.8	7.5 ± 0.2	6.6 ± 1.2	4.5 ± 1.8
Ear count	13.0 ± 1.5	17.0 ± 1.7	16.4 ± 1.5	12.4 ± 1.4	8.4 ± 2.0	7.0 ± 2.8
Grains per ear (mean)	12.9 ± 0.5	11.0 ± 0.8	12.0 ± 1.5	15.2 ± 0.9	20.2 ± 3.1	11.1 ± 3.7
Straw N exported (g)	0.17 ± 0.02	0.14 ± 0.02	0.09 ± 0.03	0.10 ± 0.01	0.09 ± 0.01	0.05 ± 0.02
Grain N exported (g)	0.17 ± 0.02	0.19 ± 0.01	0.20 ± 0.02	0.20 ± 0.01	0.17 ± 0.03	0.11 ± 0.05

Table 3. Average values of different growth parameters and N plant uptake per treatment ± standard errors (n = 5) at harvest (3rd July). Export of N in straw and grain was calculated as total N concentration in straw/grain per straw/grain biomass). Abbreviations for the biochar treatments correspond to: F_0 = fresh 0 t ha^{-1}; F_{12} = fresh 12 t ha^{-1}; F_{50} = fresh 50 t ha^{-1}; A_0 = aged 0 t ha^{-1}; A_{12} = aged 12 t ha^{-1}; A_{50} = aged 50 t ha^{-1}. The absence of letters indicates that the observed differences were not significant.

Supplementary Material

Table S1. Pig slurry characterisation. * Kjeldahl N = (organic N) + (N-NH_4); **Available N = (Kjeldahl N) - (non-hidrolisable N). w.w. stands for wet weight and d.w. for dry weight.

Parameter	Units	Value
Dry matter	% (w.w.)	86.3
pH	water, 1:5 (v/v)	6.35
Electrical conductivity	dS/m, 25ºC	51.7
Organic matter	% (w.w.)	58.3
Kjeldahl N*	% (w.w.)	5.92
Organic N	% (w.w.)	2.44
N-NH4	% (w.w.)	3.48
Non-hidrolisable N	% (w.w.)	0.99
Available N**	% (w.w.)	4.9
C/N ratio (based on organic N)		11.9
C/N ratio (based on Kjeldahl N)		4.9
P	g kg^{-1} (d.w.)	29
K	g kg^{-1} (d.w.)	38.5
Ca	g kg^{-1} (d.w.)	27.5
Mg	g kg^{-1} (d.w.)	10.6
Fe	g kg^{-1} (d.w.)	4

Table S2. Primers and thermal profiles used for real-time PCR quantification of the different target genes.

Target gene	Primers	Thermal profile	Number of cycles	Reference
nifH	nifHF nifHR	98 °C – 45 s/ 55 °C – 45 s/ 72 °C – 45 s	40	Harter et al., 2014
amoA AOA	amo19F CrenamoA16r48x	94°C, 45 s / 55°C, 45 s / 72°C, 45 s	40	Töwe et al., 2014
amoA AOB	amoA1F amoA2R	94 °C – 30 s/ 58.5 °C – 30 s/ 72 °C – 30 s	40	Harter et al., 2014
nirK	nirK876C nirK1040	95 °C – 15 s/63 °C – 30 s/72 °C – 30 s 95 °C – 15 s/58 °C – 30 s/72 °C – 30 s	6a 40	Harter et al., 2014
nosZ	nosZ2F nosZ2R	95 °C – 15 s/63-58 °C – 30 s/72 °C – 30 s 95 °C – 15 s/60 °C – 58 s/72 °C – 30 s	6a	Harter et al., 2014
nirS	nirScd3aF nirSR3cd	95 °C –15 s/ 57 °C – 30 s/ 60 °C – 15 s	40	Töwe et al., 2014
nxrB	A189 A682	94 °C –30 s/58.5 °C – 30 s/72 °C – 30 s	40	Vanparys et al., 2006

[a] touchdown -1ºC for cycle

Table S3. Summary of the results of two-way mixed ANOVAs on different variables, with treatment (biochar application rate) as between-subjects factor, and time (sampling dates) as within-subjects factor. Mixed ANOVA was conducted separately for the fresh and the aged biochar scenarios. Degrees of freedom (df) are shown as: (degrees of freedom numerator, degrees of freedom denominator); the effect size is reported as generalised eta squared (η_G^2), and significant p-values ($p < .05$) are marked in bold.

Table S3.1. Moisture

	Fresh				**Aged**			
Source	**df**	**F**	**p**	η_G^2	**df**	**F**	**p**	η_G^2
treatment	(2, 12)	11.90	**0.001**	0.38	(2, 11)	1.48	0.27	0.07
time	(4, 48)	114.93	**< .001**	0.87	(1.9, 20.3)	38.50	**< .001**	0.72
treat. x time	(8, 48)	2.40	**0.029**	0.22	(3.7, 20.3)	0.53	0.70	0.07

Table S3.2. Electrical conductivity (EC)

	Fresh				**Aged**			
Source	**df**	**F**	**p**	η_G^2	**df**	**F**	**p**	η_G^2
treatment	(2, 12)	1.75	0.22	0.06	(2, 12)	0.94	0.42	0.03
time	(4, 48)	66.13	**< .001**	0.81	(2.0, 23.5)	23.49	**< .001**	0.61
treat. x time	(8, 48)	2.37	**0.03**	0.24	(3.9, 23.5)	0.31	0.86	0.04

Table S3.3. pH

	Fresh				Aged			
Source	**df**	**F**	**p**	η_G^2	**df**	**F**	**p**	η_G^2
treatment	(2, 12)	0.30	0.74	0.02	(2, 12)	0.05	0.96	0.002
time	(4, 48)	23.26	< **.001**	0.53	(2.6, 31.4)	20.67	< **.001**	0.58
treat. x time	(8, 48)	0.67	0.72	0.06	(5.2, 31.4)	1.44	0.24	0.16

Table S3.4. Soil total Kjeldahl nitrogen (TKN)

	Fresh				Aged			
Source	**df**	**F**	**p**	η_G^2	**df**	**F**	**p**	η_G^2
treatment	(2, 12)	2.50	0.12	0.11	(2, 12)	1.54	0.26	0.11
time	(2.3, 27.9)	18.37	< **.001**	0.52	(4, 48)	16.34	< **.001**	0.40
treat. x time	(4.7, 27.9)	2.87	**0.035**	0.25	(8, 48)	1.07	0.40	0.08

Table S3.5. Soil organic carbon (C_{org})

	Fresh				Aged			
Source	**df**	**F**	**p**	η_G^2	**df**	**F**	**p**	η_G^2
treatment	(2, 12)	248.76	< **.001**	0.94	(2, 12)	54.25	< **.001**	0.87
time	(2.7, 31.8)	2.04	0.14	0.09	(4, 48)	14.21	< **.001**	0.24
treat. x time	(5.3, 31.8)	3.59	**0.01**	0.25	(8, 48)	1.49	0.18	0.06

Table S3.6. N-NO_3^- in water extracts

	Fresh				Aged			
Source	**df**	**F**	**p**	η_G^2	**df**	**F**	**p**	η_G^2
treatment	(2, 12)	1.97	0.18	0.08	(2, 12)	0.097	0.91	0.004
time	(1.9, 23.1)	116.14	**< .001**	0.88	(1.6, 13.8)	43.93	**< .001**	0.73
treat. x time	(3.8, 23.1)	2.96	**< .001**	0.27	(2.3, 13.8)	0.10	0.93	0.01

Table S3.7. N-NH_4^+ in water extracts

	Fresh				Aged			
Source	**df**	**F**	**p**	η_G^2	**df**	**F**	**p**	η_G^2
treatment	(2, 12)	0.72	0.51	0.02	(2, 12)	0.15	0.86	0.005
time	(1, 12.04)	31.50	**< .001**	0.68	(1.5, 17.9)	92.09	**< .001**	0.86
treat. x time	(2, 12.04)	0.63	0.55	0.08	(2.9, 17.9)	0.19	0.90	0.02

Table S3.8. Exchangeable N-NH_4^+ (N-NH_4^+ in KCl extracts – N-NH_4^+ in water extracts)

	Fresh				Aged			
Source	**df**	**F**	**p**	η_G^2	**df**	**F**	**p**	η_G^2
treatment	(2, 12)	0.93	0.42	0.03	(2, 12)	0.38	0.69	0.01
time	(1, 12.02)	24.08	**< .001**	0.62	(1, 12.1)	34.58	**< .001**	0.70
treat. x time	(2, 12.02)	1.05	0.38	0.12	(2, 12.1)	0.45	0.65	0.06

Table S3.9. $N\text{-}NO_2^-$ in water extracts

	Fresh				Aged			
Source	**df**	**F**	**p**	η_G^2	**df**	**F**	**p**	η_G^2
treatment	(2, 12)	1.13	0.31	0.05	(2, 12)	0.12	0.89	0.002
time	(4, 48)	30.97	**< .001**	0.67	(4, 48)	45.33	**< .001**	0.77
treat. x time	(8, 48)	1.57	0.16	0.17	(8, 48)	0.29	0.97	0.04

Table S3.10. Na^+ in water extracts

	Fresh				Aged			
Source	**df**	**F**	**p**	η_G^2	**df**	**F**	**p**	η_G^2
treatment	(2, 12)	2.76	0.10	0.12	(2, 12)	0.64	0.54	0.03
time	(4, 48)	109.9	**< .001**	0.87	(1.3, 15.9)	39.25	**< .001**	0.71
treat. x time	(8, 48)	2.51	**0.02**	0.23	(2.7, 15.9)	0.68	0.56	0.08

Table S3.11. Cl^- in water extracts

	Fresh				Aged			
Source	**df**	**F**	**p**	η_G^2	**df**	**F**	**p**	η_G^2
treatment	(2, 12)	1.83	0.20	0.06	(2, 12)	0.22	0.81	0.006
time	(2.6, 31.5)	130.99	**< .001**	0.90	(1.3, 15.1)	40.86	**< .001**	0.74
treat. x time	(5.2, 31.5)	3.91	**0.007**	0.34	(2.5, 15.1)	0.47	0.68	0.06

Table S3.12. K^+ in water extracts

	Fresh				Aged			
Source	**df**	**F**	**p**	η_G^2	**df**	**F**	**p**	η_G^2
treatment	(2, 12)	1.38	0.29	0.07	(2, 12)	2.58	0.12	0.08
time	(1.6, 18.7)	54.53	**< .001**	0.76	(1.2, 14.8)	49.81	**< .001**	0.77
treat. x time	(3.1, 18.7)	0.52	0.68	0.06	(2.5, 14.8)	1.76	0.20	0.19

Table S3.13. Ca^{2+} in water extracts

	Fresh				Aged			
Source	**df**	**F**	**p**	η_G^2	**df**	**F**	**p**	η_G^2
treatment	(2, 12)	0.70	0.52	0.03	(2, 12)	0.97	0.41	0.04
time	(2.4, 28.6)	70.40	**< .001**	0.81	(1.6, 19.7)	23.10	**< .001**	0.58
treat. x time	(4.8, 28.6)	2.24	0.08	0.21	(3.3, 19.7)	0.41	0.76	0.05

Table S3.14. Mg^{2+} in water extracts

	Fresh				Aged			
Source	**df**	**F**	**p**	η_G^2	**df**	**F**	**p**	η_G^2
treatment	(2, 12)	0.69	0.52	0.03	(2, 12)	1.58	0.25	0.04
time	(2.4, 28.3)	92.89	**< .001**	0.85	(1.3, 15.7)	39.26	**< .001**	0.74
treat. x time	(4.7, 28.3)	2.10	0.098	0.20	(2.6, 15.7)	0.34	0.78	0.04

Table S3.15. SO_4^{2-} in water extracts

	Fresh				Aged			
Source	**df**	**F**	**p**	η_G^2	**df**	**F**	**p**	η_G^2
treatment	(2, 12)	0.04	0.96	0.00	(2, 12)	1.78	0.21	0.07
time	(2.2, 26.0)	63.48	**< .001**	0.79	(2.3, 27.1)	25.74	**< .001**	0.62
treat. x time	(4.3, 26.0)	0.47	0.77	0.05	(4.5, 27.1)	1.09	0.39	0.12

Table S3.16. $N\text{-}NO_3^-$ in leachates

	Fresh				Aged			
Source	**df**	**F**	**p**	η_G^2	**df**	**F**	**p**	η_G^2
treatment	(2, 9)	0.21	0.81	0.01	(2, 11)	3.08	0.09	0.11
time	(1.7, 15.4)	50.96	**< .001**	0.83	(4, 44)	22.93	**< .001**	0.62
treat. x time	(3.4, 15.4)	0.92	0.47	0.15	(8, 44)	1.71	0.12	0.19

Table S3.17. $N\text{-}NH_4^+$ in leachates

	Fresh				Aged			
Source	**df**	**F**	**p**	η_G^2	**df**	**F**	**p**	η_G^2
treatment	(2, 9)	0.82	0.47	0.12	(2, 11)	3.12	0.09	0.12
time	(1.6, 14.6)	28.63	**< .001**	0.66	(4, 44)	29.24	**< .001**	0.67
treat. x time	(3.3, 14.6)	1.35	0.30	0.22	(8, 44)	0.59	0.78	0.07

Table S3.18. $N\text{-}NO_2^-$ in leachates

	Fresh				Aged			
Source	**df**	**F**	**p**	η_G^2	**df**	**F**	**p**	η_G^2
treatment	(2, 9)	0.20	0.83	0.01	(2, 11)	0.18	0.84	0.01
time	(1.7, 15.5)	9.08	**0.003**	0.46	(1.4, 15.2)	9.93	**0.004**	0.41
treat. x time	(3.5, 15.5)	0.64	0.62	0.11	(2.8, 15.2)	0.30	0.81	0.04

Table S3.19. Na^+ in leachates

	Fresh				Aged			
Source	**df**	**F**	**p**	η_G^2	**df**	**F**	**p**	η_G^2
treatment	(2, 9)	0.52	0.61	0.03	(2, 11)	0.98	0.41	0.04
time	(2.0, 18.3)	43.86	**< .001**	0.78	(2.1, 23.0)	18.68	**< .001**	0.56
treat. x time	(4.1, 18.3)	1.08	0.40	0.15	(4.2, 23.0)	1.82	0.16	0.20

Table S3.20. Cl^- in leachates

	Fresh				Aged			
Source	**df**	**F**	**p**	η_G^2	**df**	**F**	**p**	η_G^2
treatment	(2, 9)	0.61	0.56	0.04	(2, 11)	1.31	0.31	0.08
time	(4, 36)	61.03	**< .001**	0.83	(4, 44)	15.74	**< .001**	0.48
treat. x time	(8, 36)	2.00	0.07	0.24	(8, 44)	1.77	0.11	0.17

Table S3.21. K^+ in leachates

	Fresh				Aged			
Source	**df**	**F**	**p**	η_G^2	**df**	**F**	**p**	η_G^2
treatment	(2, 9)	2.79	0.11	0.12	(2, 11)	2.06	0.17	0.10
time	(4, 36)	22.40	**< .001**	0.66	(4, 44)	19.21	**< .001**	0.56
treat. x time	(8, 36)	1.60	0.16	0.22	(8, 44)	1.92	0.08	0.20

Table S3.22. Ca^{2+} in leachates

	Fresh				Aged			
Source	**df**	**F**	**p**	η_G^2	**df**	**F**	**p**	η_G^2
treatment	(2, 9)	0.38	0.70	0.01	(2, 11)	0.61	0.56	0.03
time	(4, 36)	11.45	**< .001**	0.51	(4, 44)	6.07	**< .001**	0.28
treat. x time	(8, 36)	1.85	0.099	0.26	(8, 44)	0.77	0.63	0.09

Table S3.23. Mg^{2+} in leachates

	Fresh				Aged			
Source	**df**	**F**	**p**	η_G^2	**df**	**F**	**p**	η_G^2
treatment	(2, 9)	2.78	0.11	0.12	(2, 11)	4.59	**0.035**	0.12
time	(4, 36)	22.40	**< .001**	0.66	(4, 44)	16.38	**< .001**	0.56
treat. x time	(8, 36)	1.60	0.16	0.22	(8, 44)	2.89	**0.01**	0.31

Table S3.24. SO_4^{2-} in leachates

	Fresh				Aged			
Source	**df**	**F**	**p**	η_G^2	**df**	**F**	**p**	η_G^2
treatment	(2, 9)	0.23	0.80	0.01	(2, 11)	3.29	0.07	0.11
time	(1.8, 15.8)	6.12	**0.01**	0.35	(1.5, 16.0)	14.27	< **.001**	0.51
treat. x time	(3.5, 15.8)	1.00	0.43	0.15	(2.9, 16.0)	1.88	0.17	0.21

Table S3.25. Dissolved organic carbon in K_2SO_4 extracts (DOC)

	Fresh				Aged			
Source	**df**	**F**	**p**	η_G^2	**df**	**F**	**p**	η_G^2
treatment	(2, 12)	0.58	0.57	0.01	(2, 12)	0.22	0.80	0.01
time	(1.7, 20.1)	7.41	**0.006**	0.35	(4, 48)	5.34	**0.001**	0.27
treat. x time	(3.4, 20.1)	1.24	0.32	0.15	(8, 48)	1.15	0.35	0.14

Table S3.26. Dissolved organic nitrogen in K_2SO_4 extracts (DON)

	Fresh				Aged			
Source	**df**	**F**	**p**	η_G^2	**df**	**F**	**p**	η_G^2
treatment	(2, 12)	0.15	0.86	0.01	(2, 12)	0.36	0.70	0.01
time	(2, 24)	27.92	< **.001**	0.57	(1.4, 17.3)	39.10	< **.001**	0.72
treat. x time	(4, 24)	1.32	0.29	0.11	(2.9, 17.3)	0.39	0.76	0.05

Table S3.27. Microbial biomass carbon (C_{mic})

	Fresh				Aged			
Source	**df**	**F**	**p**	η_G^2	**df**	**F**	**p**	η_G^2
treatment	(2, 12)	0.02	0.98	0.00	(2, 12)	2.56	0.12	0.07
time	(1.9, 22.5)	7.21	**0.004**	0.33	(2.5, 30.4)	2.44	0.09	0.14
treat. x time	(3.7, 22.5)	0.62	0.64	0.08	(5.1, 30.4)	1.31	0.28	0.15

Table S3.28. Microbial biomass nitrogen (N_{mic})

	Fresh				Aged			
Source	**df**	**F**	**p**	η_G^2	**df**	**F**	**p**	η_G^2
treatment	(2, 12)	2.19	0.16	0.11	(2, 12)	1.15	0.35	0.06
time	(2, 24)	10.35	**< .001**	0.36	(3, 36)	6.00	**0.002**	0.26
treat. x time	(4, 24)	0.87	0.50	0.09	(6, 36)	0.81	0.57	0.09

Table S3.29. Soil basal respiration (BAS)

	Fresh				Aged			
Source	**df**	**F**	**p**	η_G^2	**df**	**F**	**p**	η_G^2
treatment	(2, 12)	3.75	0.054	0.14	(2, 12)	1.23	0.33	0.04
time	(4, 48)	7.97	**< .001**	0.33	(4, 48)	13.68	**< .001**	0.47
treat. x time	(8, 48)	1.69	0.13	0.17	(8, 48)	1.66	0.13	0.18

Table S3.30. N-N_2O emission rate

	Fresh				Aged			
Source	**df**	**F**	**p**	η_G^2	**df**	**F**	**p**	η_G^2
treatment	(2, 2)	4.47	0.18	0.62	(2, 2)	13.46	0.06	0.66
time	(4, 8)	257.01	**< .001**	0.99	(4, 8)	43.09	**< .001**	0.95
treat. x time	(8, 8)	9.72	**0.002**	0.86	(8, 8)	5.47	**0.01**	0.82

Table S3.31. C-CO_2 emission rate

	Fresh				Aged			
Source	**df**	**F**	**p**	η_G^2	**df**	**F**	**p**	η_G^2
treatment	(2, 2)	6.39	0.14	0.56	(2, 2)	0.39	0.72	0.05
time	(4, 8)	131.96	**< .001**	0.98	(4, 8)	12.83	**0.001**	0.85
treat. x time	(8, 8)	4.46	**0.025**	0.78	(8, 8)	0.09	1.00	0.07

Table S3.32. N-NH_3 emission rate

	Fresh				Aged			
Source	**df**	**F**	**p**	η_G^2	**df**	**F**	**p**	η_G^2
treatment	(2, 12)	2.87	0.096	0.14	(2, 12)	2.70	0.10	0.17
time	(1.5, 17.5)	28.40	**< .001**	0.61	(3, 36)	28.93	**< .001**	0.57
treat. x time	(2.9, 17.5)	0.99	0.42	0.10	(6, 36)	1.73	0.14	0.14

Table S3.33. δ^{15}N-NO_3^- in soil KCl extracts

	Fresh				Aged			
Source	**df**	**F**	**p**	η_G^2	**df**	**F**	**p**	η_G^2
treatment	(1, 8)	0.03	0.86	0.00	(1, 8)	1.00	0.35	0.02
time	(4, 32)	30.72	**< .001**	0.69	(4, 32)	29.97	**< .001**	0.77
treat. x time	(4, 32)	0.16	0.96	0.01	(4, 32)	1.41	0.25	0.13

Table S3.34. δ^{18}O-NO_3^- in soil KCl extracts

	Fresh				Aged			
Source	**df**	**F**	**p**	η_G^2	**df**	**F**	**p**	η_G^2
treatment	(1, 8)	0.44	0.53	0.02	(1, 8)	1.99	0.20	0.06
time	(4, 32)	0.88	0.49	0.06	(4, 32)	1.94	0.13	0.15
treat. x time	(4, 32)	1.56	0.21	0.1	(4, 32)	0.35	0.84	0.03

Table S3.35. δ^{15}N-NO_3^- in leachates

	Fresh			
Source	**df**	**F**	**p**	η_G^2
treatment	(1, 6)	1.21	0.31	0.10
time	(4, 24)	13.82	**< .001**	0.52
treat. x time	(4, 24)	2.15	0.11	0.15

Table S3.36. δ^{18}O-NO_3^- in leachates

	Fresh			
Source	**df**	**F**	**p**	η_G^2
treatment	(1, 6)	7.53	**0.034**	0.22
time	(4, 24)	1.30	0.29	0.15
treat. x time	(4, 24)	0.66	0.63	0.08

Table S4. Nutrient content in grain and straw of harvested barley. Reported values are mean ± standard errors (n = 5). Abbreviations for the biochar treatments correspond to: F_0 = fresh 0 t ha^{-1}; F_{12} = fresh 12 t ha^{-1}; F_{50} = fresh 50 t ha^{-1}; A_0 = aged 0 t ha^{-1}; A_{12} = aged 12 t ha^{-1}; A_{50} = aged 50 t ha^{-1}. The absence of letters indicates that there were no significant differences.

	Nutrient	**Treatment**					
		F_0	**F_{12}**	**F_{50}**	**A_0**	**A_{12}**	**A_{50}**
Grain	P (%)	0.83 ± 0.0	0.86 ± 0.0	0.83 ± 0.0	0.83 ± 0.0	0.81 ± 0.0	0.84 ± 0.0
	K (%)	1.07 ± 0.1	1.13 ± 0.1	1.05 ± 0.0	1.06 ± 0.1	1.10 ± 0.1	1.05 ± 0.1
	Ca (%)	0.12 ± 0.0	0.10 ± 0.0	0.10 ± 0.0	0.09 ± 0.0	0.06 ± 0.0	0.09 ± 0.0
	Mg (%)	0.13 ± 0.0	0.14 ± 0.0	0.13 ± 0.0	0.14 ± 0.0	0.14 ± 0.0	0.14 ± 0.0
	S (%)	0.06 ± 0.0	0.07 ± 0.0	0.07 ± 0.0	0.05 ± 0.0	0.04 ± 0.0	0.05 ± 0.0
	Mn (mg kg^{-1})	2.00 ± 0.0	1.87 ± 0.1	1.82 ± 0.1	1.90 ± 0.1	1.84 ± 0.1	1.87 ± 0.1
	Zn (mg kg^{-1})	6.11 ± 0.1	6.54 ± 0.4	6.10 ± 0.1	6.05 ± 0.2	6.02 ± 0.2	5.88 ± 0.1
Straw	P (%)	0.05 ± 0.0	0.07 ± 0.0	0.05 ± 0.0	0.07 ± 0.0	0.17 ± 0.1	0.30 ± 0.1
	K (%)	1.18 ± 0.2	1.35 ± 0.3	1.36 ± 0.1	1.61 ± 0.3	1.63 ± 0.4	1.88 ± 0.5
	Ca (%)	0.28 ± 0.1	0.31 ± 0.0	0.29 ± 0.0	0.29 ± 0.1	0.31 ± 0.1	0.19 ± 0.0
	Mg (%)	0.0 ± 0.0	0.0 ± 0.0	0.0 ± 0.0	0.0 ± 0.0	0.0 ± 0.1	0.0 ± 0.1
	S (%)	0.30 ± 0.0	0.29 ± 0.0	0.28 ± 0.0	0.29 ± 0.0	0.31 ± 0.0	0.32 ± 0.0
	Mn (mg kg^{-1})	4.22 ± 0.5	4.22 ± 0.2	3.98 ± 0.4	3.45 ± 0.1	3.76 ± 0.2	3.87 ± 0.4
	Zn (mg kg^{-1})	3.34 ± 0.1	3.60 ± 0.0	3.53 ± 0.1	3.50± 0.2	3.63 ± 0.2	4.19 ± 0.5

Table S5. Mean values of *Folsomia candida* adult survival (%) and juvenile number per treatment ± standard errors (n = 5) at the onset of the experiment. Abbreviations for the biochar treatments correspond to: F_0 = fresh 0 t ha^{-1}; F_{12} = fresh 12 t ha^{-1}; F_{50} = fresh 50 t ha^{-1}; A_0 = aged 0 t ha^{-1}; A_{12} = aged 12 t ha^{-1}; A_{50} = aged 50 t ha^{-1}. The absence of letters indicates that the observed differences were not significant.

Parameter	**Treatment**					
	F_0	**F_{12}**	**F_{50}**	**A_0**	**A_{12}**	**A_{50}**
Adult survival (%)	86 ± 5.1	86 ± 10.3	76 ± 10.3	88 ± 4.9	94 ± 4.0	90 ± 4.5
Juvenile number	574.6 ± 97.5	517 ± 22.0	438 ± 45.0	552.8 ± 59.9	512.4 ± 52.0	540.2 ± 29.2

Table S6. *Raphidocelis subcapitata* yield inhibition (%) at four elutriate concentrations (C): 81.6, 51, 30.6, and 10.2%. Abbreviations for the biochar treatments correspond to: F_0 = fresh 0 t ha^{-1}; F_{12} = fresh 12 t ha^{-1}; F_{50} = fresh 50 t ha^{-1}; A_0 = aged 0 t ha^{-1}; A_{12} = aged 12 t ha^{-1}; A_{50} = aged 50 t ha^{-1}. Values are averages per treatment ± standard errors (n = 5) at the onset of the experiment. The absence of letters indicates that the observed differences were not significant.

Parameter	**C% elutriate**	**Treatment**					
		F_0	**F_{12}**	**F_{50}**	**A_0**	**A_{12}**	**A_{50}**
Yield inhibition (%)	10.2	-1.3 ± 1	0.4 ± 0.6	8.1 ± 9	11.6 ± 7.6	-1.6 ± 0.5	7.2 ± 6.1
	30.6	-4.8 ± 3.3	-4 ± 1	-4 ± 1.3	1.9 ± 6.3	-4.4 ± 2.1	-4.9 ± 1.1
	51	-5.8 ± 0.4	-3.6 ± 1.4	-5.4 ± 0.2	1.8 ± 6.1	-2.4 ± 1.7	-2.4 ± 1
	81.6	-2.2 ± 0.5	-2.9 ± 1.3	5.7 ± 9.4	-3.4 ± 1.1	-2.6 ± 1.9	-2 ± 0.7

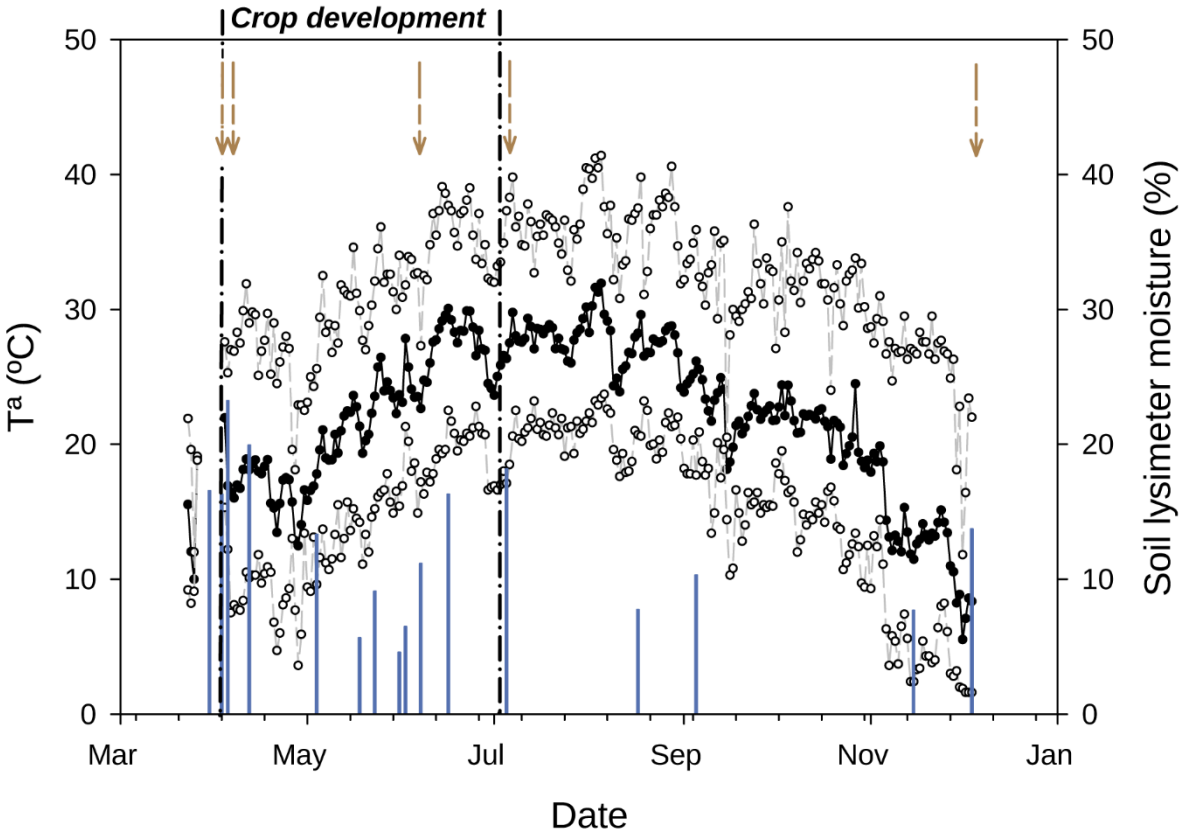

Figure S1. Record of greenhouse's mean daily temperature (filled dots), maximum and minimum daily temperature (empty dots), and soil lysimeters moisture (%) measured gravimetrically (blue bars). The brown arrows indicate the sampling dates and dash-dotted lines indicate the period ranging from fertilisation and sowing events (first line) and harvest (second line), thus covering the period of barley crop development. Temperature data has been provided by IRTA-Torre Marimon.

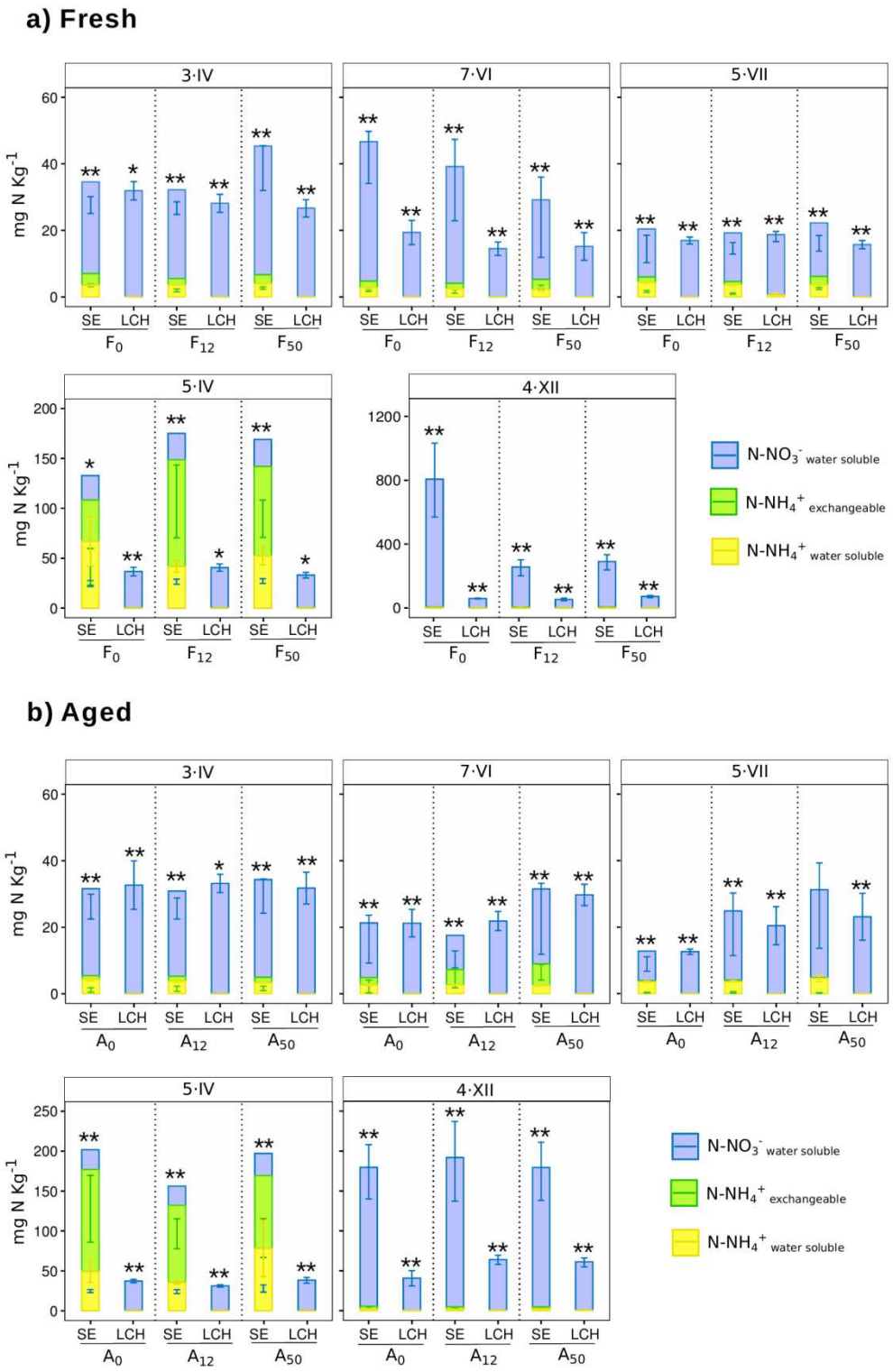

Figure S2. $N\text{-}NO_3^-$ and $N\text{-}NH_4^+$ (mg kg^{-1} DW soil) evolution in soil extracts (SE) and leachates (LCH) along five different samplings (3·IV = 3rd April; 5·IV = 5th April; 7·VI = 7th June; 5·VII = 5th July and 4·XII = 4th December) in a) fresh biochar scenario and b) aged biochar scenario. Abbreviations for the biochar treatments correspond to: F_0 = fresh 0 t ha^{-1}; F_{12} = fresh 12 t ha^{-1}; F_{50} = fresh 50 t ha^{-1}; A_0 = aged 0 t ha^{-1}; A_{12} = aged 12 t ha^{-1}; A_{50} = aged 50 t ha^{-1}. Bars correspond to mean values and error bars represent standard error

(n = 5). Asterisks indicate statistically significant differences between $N\text{-}NO_3^-$ and $N\text{-}NH_4^+$ within each soil extract or leachate (* = $p < 0.05$, ** = $p < 0.01$). For soil extracts comparisons were made between $N\text{-}NO_3^-$ (water soluble) and total $N\text{-}NH_4^+$ (exchangeable + water soluble) while in leachates water soluble concentrations of $N\text{-}NO_3^-$ and $N\text{-}NH_4^+$ were compared.

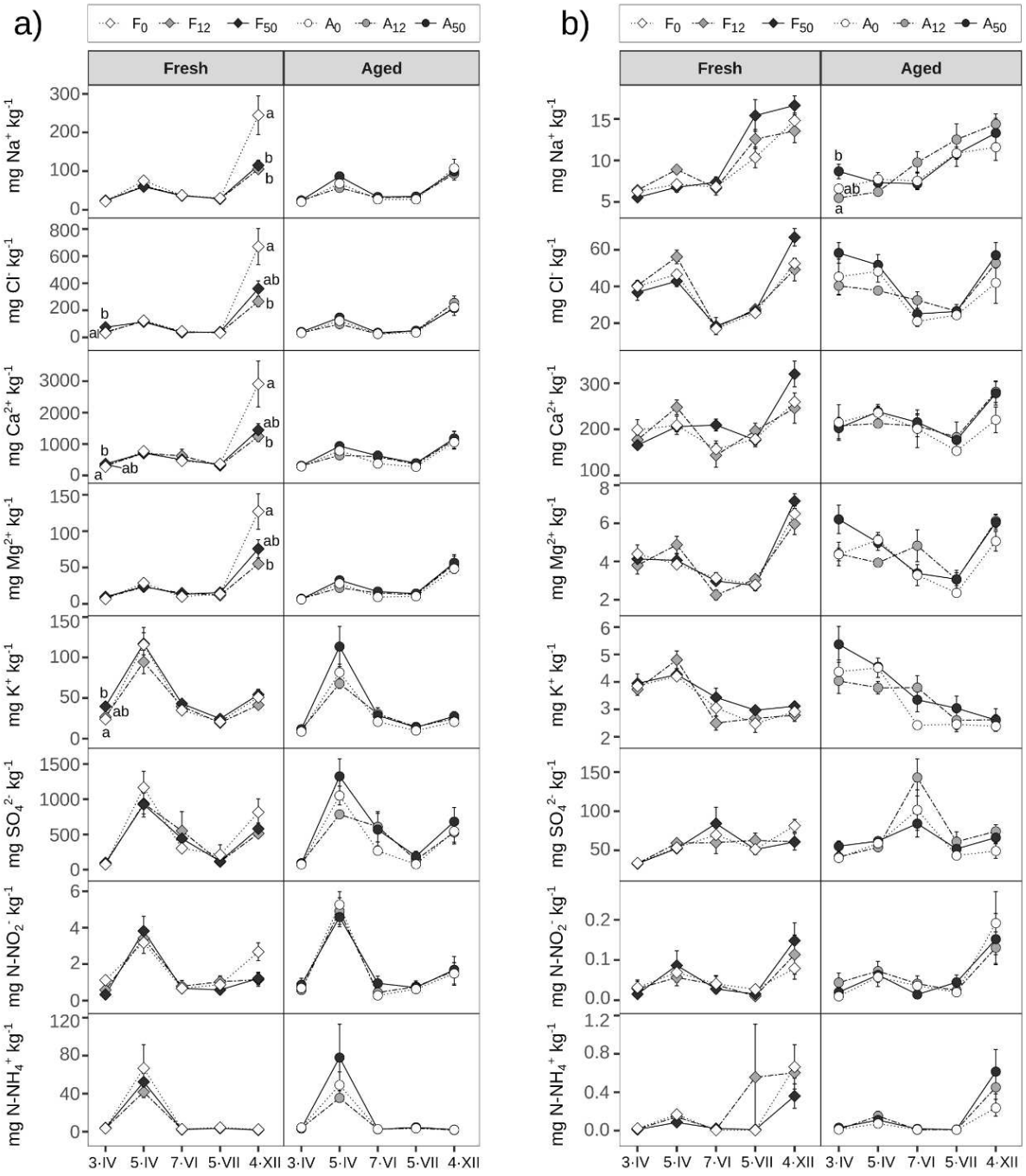

Figure S3. Ionic concentrations (mg kg^{-1} DW soil) evolution in water extracts (a) and leachates (b) along five different samplings (3·IV = 3rd April; 5·IV = 5th April; 7·VI = 7th June; 5·VII = 5th July and 4·XII = 4th December). Abbreviations for the biochar treatments correspond to: F_0 = fresh 0 t ha^{-1}; F_{12} = fresh 12 t ha^{-1}; F_{50} = fresh 50 t ha^{-1}; A_0 = aged 0 t ha^{-1}; A_{12} = aged 12 t ha^{-1}; A_{50} = aged 50 t ha^{-1}. Symbols represent the mean values, and bars represent the corresponding standard error (n = 5). Different letters indicate statistically significant differences between treatments within a particular sampling.

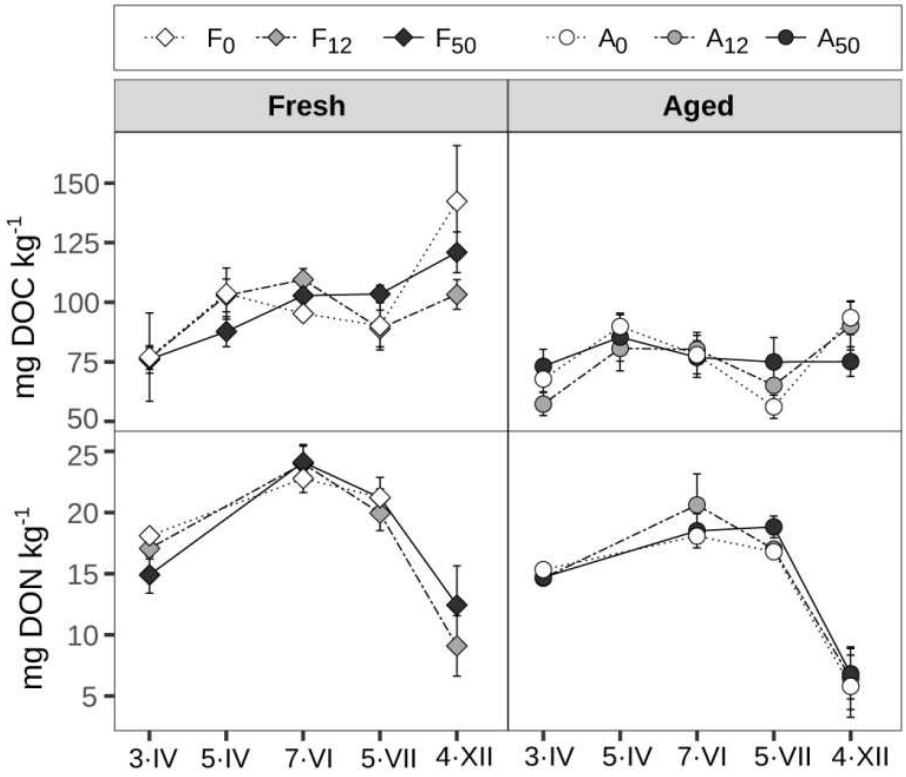

Figure S4. DOC and DON concentrations (mg kg^{-1} DW soil) evolution in water extracts along five different samplings (3·IV = 3rd April; 5·IV = 5th April; 7·VI = 7th June; 5·VII = 5th July and 4·XII = 4th December). Note that DON for the 5·IV sampling (both fresh and aged scenarios) and for F_0 at 4·XII is not shown as its calculation was not possible. Abbreviations for the biochar treatments correspond to: F_0 = fresh 0 t ha^{-1}; F_{12} = fresh 12 t ha^{-1}; F_{50} = fresh 50 t ha^{-1}; A_0 = aged 0 t ha^{-1}; A_{12} = aged 12 t ha^{-1}; A_{50} = aged 50 t ha^{-1}. Symbols represent the mean values, and bars represent the corresponding standard error (n = 5). The absence of letters indicates that the observed differences were not significant.

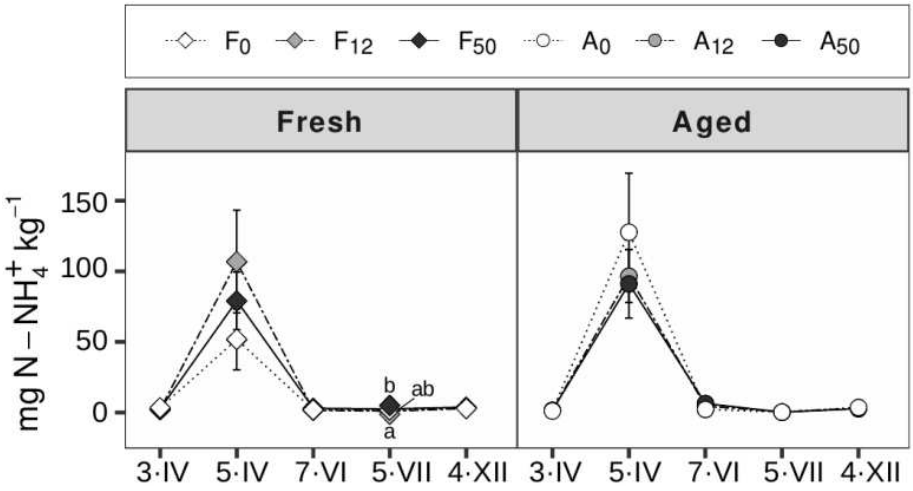

Figure S5. Exchangeable N-NH_4^+ (mg kg^{-1} DW soil), measured as KCl extractable N-NH_4^+ concentrations minus soluble N-NH_4^+ concentrations, along five different samplings (3·IV = 3rd April; 5·IV = 5th April; 7·VI = 7th June; 5·VII = 5th July and 4·XII = 4th December). Abbreviations for the biochar treatments correspond to: F_0 = fresh 0 t ha^{-1}; F_{12} = fresh 12 t ha^{-1}; F_{50} = fresh 50 t ha^{-1}; A_0 = aged 0 t ha^{-1}; A_{12} = aged 12 t ha^{-1}; A_{50} = aged 50 t ha^{-1}. Symbols represent the mean values, and bars represent the corresponding standard error (n = 5). Different letters indicate statistically significant differences among treatments for a specific sampling. Means ± SE at 5·VII for the fresh biochar scenario were: F_0 = 1.63 ± 0.29 mg kg^{-1}, F_{12} = 1.00 ± 0.20 mg kg^{-1}, and F_{50} = 2.53 ± 0.31 mg kg^{-1}.

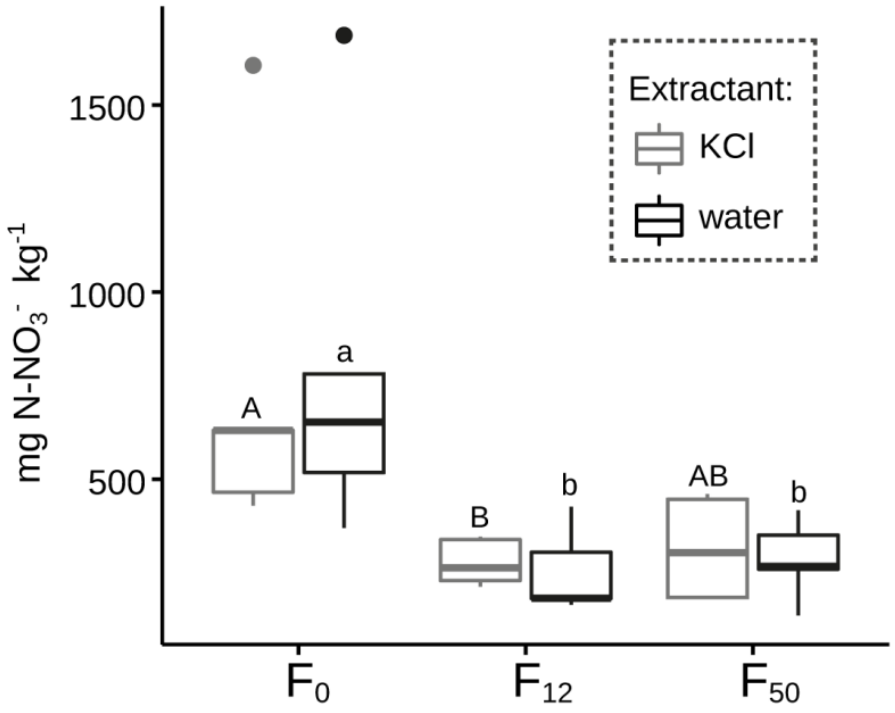

Figure S6. KCl-extractable and soluble (water extract) $N\text{-}NO_3^-$ content (mg kg^{-1} DW soil) at the 4th December, 2017 sampling date (bare soil sampling). Abbreviations for the biochar treatments correspond to: F_0 = fresh 0 t ha^{-1}; F_{12} = fresh 12 t ha^{-1}; F_{50} = fresh 50 t ha^{-1}. Different uppercase letters indicate statistical significance between treatments (F_0, F_{12} and F_{50}) within the KCl extracts, while lowercase letters indicate differences within the water extracts ($p<0.05$). There were no statistical differences between KCl and water extracts on each treatment.

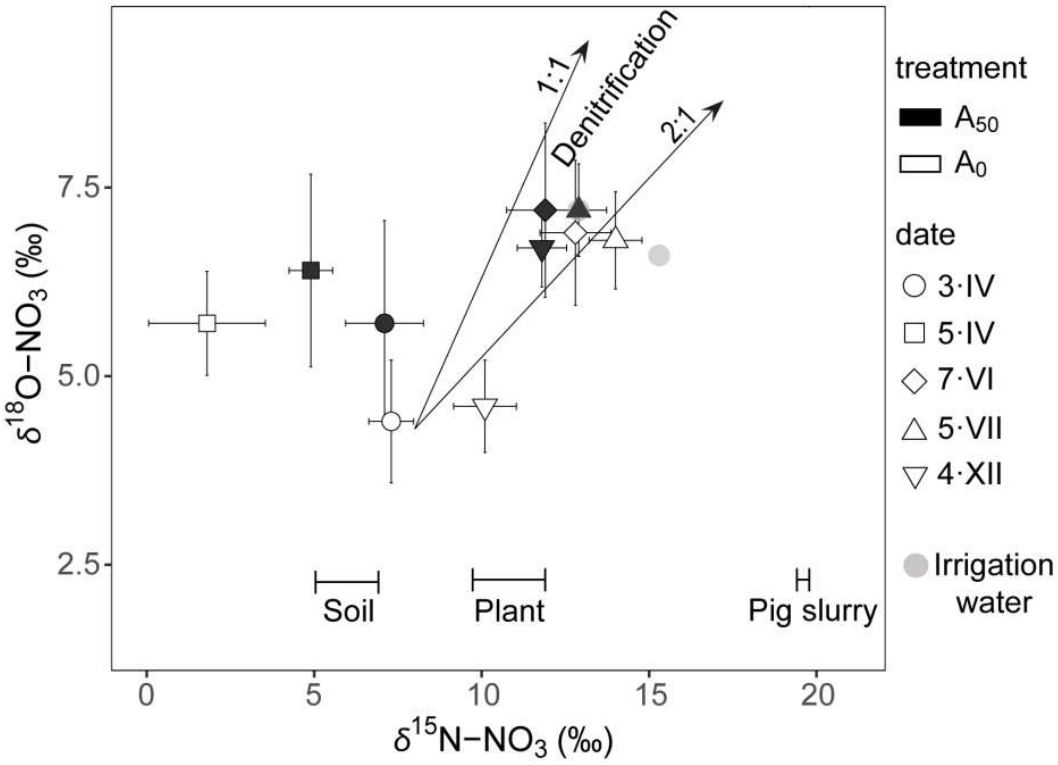

Figure S7. $\delta^{18}O$ and $\delta^{15}N$ of nitrate measured in KCl extracts for the aged scenario along five different samplings (3·IV = 3rd April; 5·IV = 5th April; 7·VI = 7th June; 5·VII = 5th July and 4·XII = 4th December). Symbols with error bars represent the mean values and standard error (n = 5) respectively. The two arrows indicate typical expected slopes for values resulting from denitrification. Abbreviations for the biochar treatments correspond to: A_0 = aged 0 t ha^{-1}; A_{50} = aged 50 t ha^{-1}. $\delta^{15}N$ of soil, harvested plants (from fresh scenario) and pig slurry, and also $\delta^{15}N$ vs $\delta^{18}O$ of dissolved NO_3^- from irrigation water are shown.

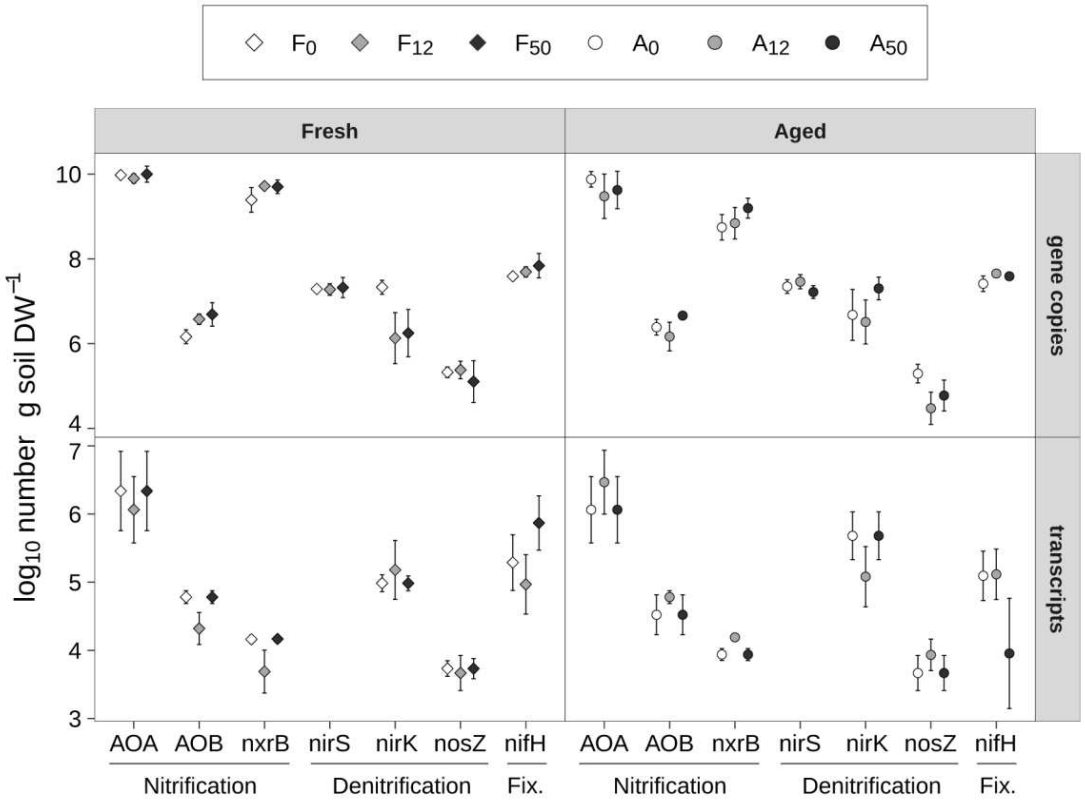

Figure S8. Gene copies and transcripts for enzymes that catalyse processes of the nitrogen cycle (nitrification, denitrification, and fixation) on 12th April, 2017 (9 days after fertilisation). nirS transcripts were not detectable and thus are not shown. Abbreviations for the biochar treatments correspond to: F_0 = fresh 0 t ha^{-1}; F_{12} = fresh 12 t ha^{-1}; F_{50} = fresh 50 t ha^{-1}; A_0 = aged 0 t ha^{-1}; A_{12} = aged 12 t ha^{-1}; A_{50} = aged 50 t ha^{-1}. Symbols represent the mean values, and bars represent the corresponding standard error (n = 5). The absence of letters indicates that the observed differences were not significant.